Parametric Analysis for Magnetorheological Finishing of External Cylindrical Surface of C60 Steel using Solid Rotating Tool Core

A dissertation submitted in partial fulfilment of requirement for the award of degree of

Master of Engineering
in
Production Engineering

by

Ashpreet Singh

Roll No.: 801585005

Under the guidance of

Dr. ANANT KUMAR SINGH

Assistant Professor

MECHANICAL ENGINEERING DEPARTMENT

THAPAR UNIVERSITY

PATIALA (PB), INDIA, 147004

July, 2017

CERTIFICATE

I hereby declare that the work done in this thesis entitled "**Parametric Analysis for Magnetorheological Finishing of External Cylindrical Surface of C60 Steel using Solid Rotating Tool Core**" is an authentic record of my work carried out as requirements for the award of the degree of **Master of Engineering** in **Production Engineering** at **Thapar University, Patiala** under the supervision of **Dr. Anant Kumar Singh**, Assistant Professor, Mechanical Engineering Department, Thapar University, Patiala during July, 2015 to July, 2017. No part of the matter embodied in this report has been submitted to any other university or institute for the award of any degree.

Dated: 10/08/2017

Ashpreet Singh

Ashpreet Singh

Roll No.: 801585005

This is to certify that above statement made by the student concerned is correct to the best of my knowledge and belief.

10/08/2017

Dr. Anant Kumar Singh

Assistant Professor

Mechanical Engineering Department

Thapar University, Patiala

Dedicated to

My Mother

Acknowledgements

It is indeed a pleasure for me to express my sincere gratitude to those who have always helped me for this dissertation work. I sincerely convey my gratitude to my thesis guide **Dr. Anant Kumar Singh** who made me believe in myself and guided me through the whole process of dissertation writing. He has never failed to help me to get a grasp on the subject. I am sure that this dissertation would not have been possible without his support, understanding and encouragement.

I am also thankful to **Dr. S. K. Mahopatra,** Head of Department, MED, as well as **Dr. Vinod Kumar Singla,** P.G. Coordinator, MED, for providing us with the adequate infrastructure in carrying the work. I would like to thank the entire faculty and staff of Mechanical Engineering Department and my friends who devoted their valuable time and help me in all possible ways towards successful completion of this work. My sincere thanks to the whole staff of Central Workshop for their valuable co-operation. I thanks all those who have contributed directly or indirectly to this work.

Lastly, I would like to thanks my family member for their years of guidance, support, and encouragement. It would not possible without them to reach up to this point. They have always wanted the best for me and I admire their determination and sacrifices.

Ashpreet Singh

(Ashpreet Singh)

Abstract

A magnetorheological fluid based finishing process has been used to finish the external cylindrical surfaces at nano-level more efficiently. The existing MR finishing process based on stationary curved core tool tip is found comparatively less effective than the present process based on a rotating flat core tool tip for finishing the external cylindrical surfaces. This is due to the fact that in present process both workpiece and tool are rotating rather than giving rotation to the workpiece alone as in existing process. The carbonyl iron particles (CIPs) chains are rotated along with the rotation of the tool. This results in increase in kinetic energy of the active abrasive particles gripped by CIPs chains which causes for the better finishing performance. In preliminary experiment, finishing is done by both the tool tips namely, stationary curved core tool tip and rotating flat core tool tip. The final outcomes and results of the process using both these tool tips are compared. The R_a, R_q and R_z are reduced to 71.62%, 72.53% and 70.73% with stationary curved core tool tip, and 94.59%, 94.51% and 92.68% with rotating flat core tool tip in 90 minutes of MR finishing. The overall results revealed that the present developed process using rotating flat tool tip is more useful in finishing of external cylindrical surfaces as compared to the stationary curved tool tip. The shafts made of steel of grade C60 is taken as workpiece which finds application in manufacturing of various automobile components such as crankshafts, rocker arm shafts and rack-pinion power steering tie rods. In this research, detailed study through statistical design of the experiments is conducted by the developed rotating flat solid core based electromagnetic tool. Response surface methodology (RSM) has been used to plan and analyze the effect of current, tool rotational speed, workpiece rotational speed and abrasives concentration on percentage reduction in surface roughness ($\%\Delta R_a$). The experimental outcomes are discussed and the finishing parameters are optimized to obtain the best finishing results. Analysis of the experimental data showed that the percentage reduction in surface roughness was highly influenced by the supplied current and tool rotational speed which are followed by workpiece rotational speed and abrasives concentration. This confirmed the significant role of tool rotation in present developed process for the excessive finishing performance which was not there in the existing nanofinishing process. The surface finish was obtained as low as 52 nm from the initial value of about 350 nm in 30 minutes of finishing time with the optimized parameters.

Keywords: External cylindrical surfaces; Fine finishing processes; magnetorheological nano-finishing; Rotating core tool; Automobile components; C60 steel.

Contents

List of figures

List of tables

Nomenclature

R_a = Average roughness value (µm)

R_z = Average distance between the highest peak and the lowest valley in each sampling length (µm)

R_q = Root mean square value (µm)

R_{ai} = Initial average roughness value (µm)

R_{af} = Final average roughness value (µm)

ΔR_a = change in average roughness value (µm)

$\% \Delta R_a$ = Percentage reduction in surface roughness

F_1 = Tangential force acted by the abrasive particle on the workpiece surface due to the rotation of tool (N)

F_2 = Tangential force acted by the workpiece surface on the abrasive particle due to the rotation of the workpiece (N)

Greek Symbols

µ = Micro

μ_0 = Absolute permeability of free space

Acronyms

I = Current

T = Rotation speed of tool core

W =Rotational speed of workpiece

A = Abrasive particles concentration

AISI = American Iron and Steel Institite

RMS = Root mean square

DoF = Degree of freedom

FMAB = Flexible magnetic abrasive brush

SAE = Society of automotive Engineers

2FI = Two factor interaction

S.D. = Standard deviation

C.V. = Coefficient of variance

C.I. = Confidence interval

VIF = Variance inflection factor

CIP = Carbonyl iron particles

MAF = Magnetic abrasive finishing

MRF = Magnetorheological finishing

MRP = Magnetorheological polishing

MRR = Material removal rate

SEM = Scanning electron microscope

CCD = Central Composite Design

RSM = Response surface method

ANOVA= Analysis of Variance

Chapter 1
Introduction

1.1 Introduction

The surface finish corresponds to a vital & valuable phase of the overall production system. This process is laborious and uncontrollable in the production of precise components as it requires as much as 15% of the total production cost [Bedi and Singh, 2016]. For the production of critical cylindrical parts, the process of converting raw materials into finished components can be divided into two categories which are material conversion process and abrasive finishing process respectively as shown in the Fig. 1.1. Material conversion processes include forming or forging, various material removal processes (like turning, boring, drilling, etc.) and heat treatment processes (if applied) which are necessary to control the microstructural and mechanical properties of machined components whereas abrasive finishing processes include grinding and other finishing technologies which will be explained in detail later [Hashimoto *et al*., 2016].

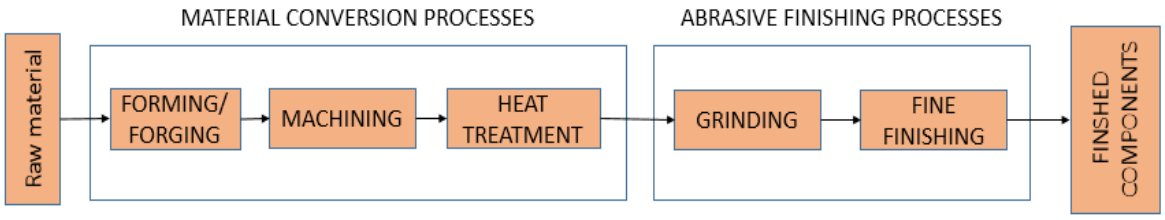

Figure 1.1: Typical manufacturing process from raw material to finished component [Hashimoto *et al.*, 2016]

1.2 Classification of Abrasive Finishing Processes

The classification of the abrasive finishing technologies used for the external cylindrical surfaces is shown in the Fig. 1.2. As shown, these are divided in two categories: - motion-copying processes and pressure copying processes. Motion Copying process remove material to a given depth of cut which results in controlling dimensional accuracy. Grinding process using bonded abrasive wheel is an example of this type. But on the other hand, pressure copying process has no specified depth of cut but removes material via pressure of the tool against the workpiece. This results in improving desired surface geometries and surface integrities instead of improving dimensional accuracy. Further, abrasive fine finishing

technologies can be divided accordingly as (i) Abrasive state, (ii) tools used for the processes, (iii) Finishing methods. Processes are of two types on the basis of abrasive state i.e. bonded and unbonded. In the bonded-abrasive state, the abrasive participates in machining while remaining fixed in a matrix. This category includes abrasive stone and coated abrasive. Abrasive stones consist of abrasive grains, a bonding agent, and pores. Abrasive stones are used in honing and superfinishing. Coated abrasives are composed of abrasive grains bonded to a flexible substrate using adhesives. Common substrates include vulcanized fibre, cloth, plastic tapes, plastic films and nylon brushes. Coated abrasives are used in film/tape/sandpaper/ finishing and brushing. In the unbonded state, the abrasives freely participates in finishing. The tools used for this purpose are abrasive slurry and abrasive flow media. Abrasive slurries are used in lapping. Abrasive flow media are used in magnetic abrasive finishing (MAF) and magnetorheological finishing (MRF). In MRF, abrasive grains mixed with ferromagnetic particles (such as iron particles) are suspended in base fluid which is either water or paraffin oil and grease [Hashimoto *et al.*, 2016].

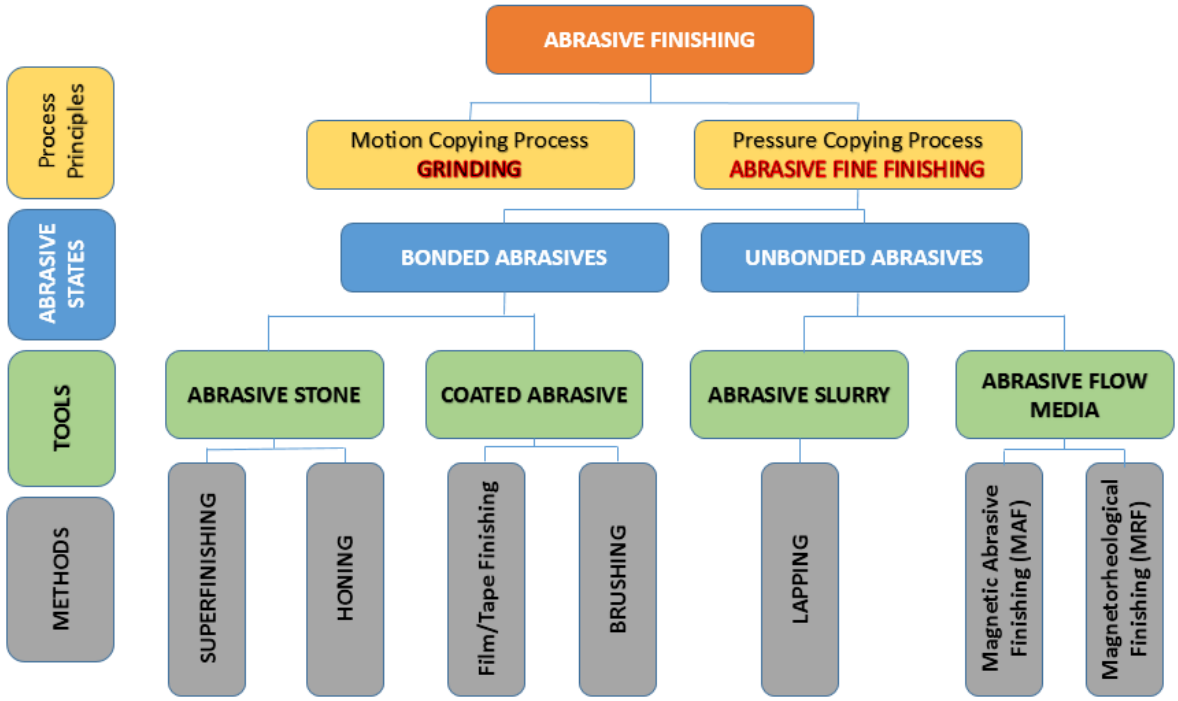

Figure 1.2: Classification of Abrasive Finishing technology [Hashimoto *et al.*, 2016]

1.2.1 Grinding

In industries, grinding processes are responsible for obtaining the precision of most of the functional parts. These processes have high specific energy in comparison to the others

available processes. The reasons for having high specific energy are the small size of chip and also all the grains do not participate in cutting, some are ploughing or deforming the workpiece while others are rubbing at the surface of the workpiece [Jermolajev *et al.*, 2015]. Moreover, the friction between wheel and the workpiece is responsible for the temperature rising of the workpiece [Alonso *et al.*, 2015]. Due to this temperature rise, a hardened surface layer is created [Nguyen and Zhang, 2011]. This thermo-mechanical technique that uses stress induced heat in grinding is also known as Grinding-hardening [Liu *et al.*, 2015]. It has been proved that wear resistance and fatigue strength of grinding hardened layer sample is much more than that of a conventional heat-treated sample [Zarudi and Zhang, 2002]. To know the profile generation of hardened layers, it is better to obtain the trajectories of grinding-induced heat sources which may be determined by grinding configurations. In surface grinding configuration, the heat source moves along a linear feeding direction [Foeckerer *et al.*, 2013] whereas in cylindrical grinding configuration, the analysis becomes somewhat difficult. For example in traverse cylindrical grinding, the overlapping of sequential passes results in a non-uniform hardened layer along the axial direction of cylinder [Nguyen *et al.*, 2014]. The transverse and plunge grinding configuration is shown in the Fig. 1.3. However in plunge grinding, the way of the wheel-work engagement could largely influence the uniformity of the hardened layer [Hyatt *et al.*, 2013].

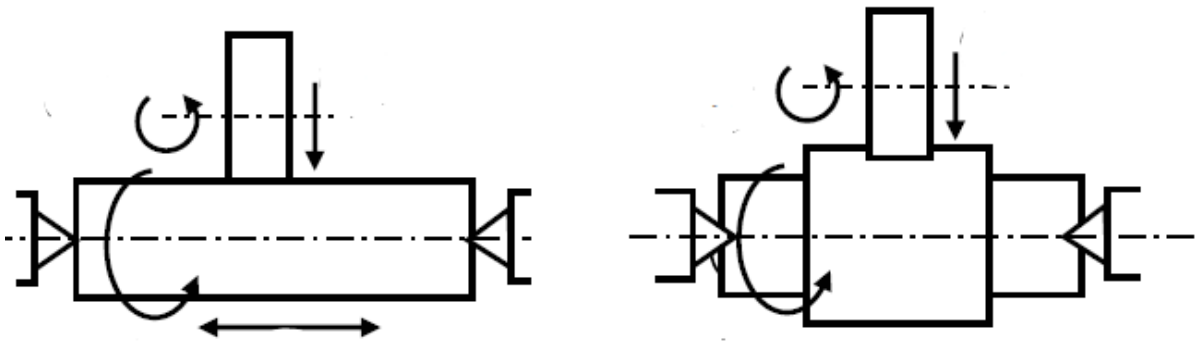

Figure 1.3: Cylindrical (a) traverse grinding and (b) plunge grinding [Liu *et al.*, 2015]

Sometimes poor dissipation of grinding heat could lead to surface defects (eg. Micro fracture, burns and unfavorable residual stresses) (Malkin and Guo, 2007). To avoid this, Textured Grinding Wheels TGWs have been developed. These are specially designed wheels that have both active and passive grinding areas. The active area performs the grinding

process whereas passive area act as reservoirs to transport more coolants/lubricants into the grinding zone [Li and Axinte, 2016].

1.2.2 Lapping

In this process, abrasive slurry act as finishing media which is circulated in between the workpiece and tool (lap). This circulation is done by the relative motion in between the tool and the workpiece and also an additional finishing pressure is applied on the tool. Lapping may be two or three body mechanism depending on whether the interaction between abrasive and the workpiece is rolling or sliding. Rolling abrasives cause micro-cracks and breakout of surface particles and thus are responsible for the material removal [Evans *et al*., 2003]. This process mainly consists of 4 components system: granule, workpiece, carrier fluid & platen as shown in the figure. It has been proved that lapping pressure, lapping time and abrasive grain size are the dominating variables in this process [Kim and Choi, 1995].

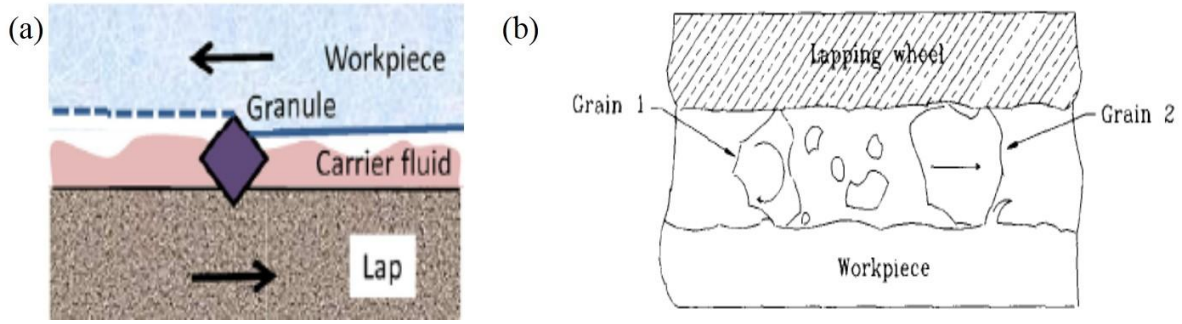

Figure 1.4: Lapping process (a) components [Hashimoto et al, 2016], and (b) Model of the abrasives acting on the workpiece [Kim *et al.*, 1995]

1.2.3 Superfinishing

Superfinishing employs abrasive stone or tape, which is held against the surface of the rotating work with a controlled contact pressure, and moves with a rapid short-stroke oscillation perpendicular to the work rotational direction. This results in the sinusoidal movement of the tool as shown in the Fig. 1.5 [Chang *et al.,* 2008]. Superfinishing improves surface finish with crosshatch patterns, geometrical accuracy, and workpiece specifications such as profile accuracy and roundness [Hashimoto *et al.*, 2016].

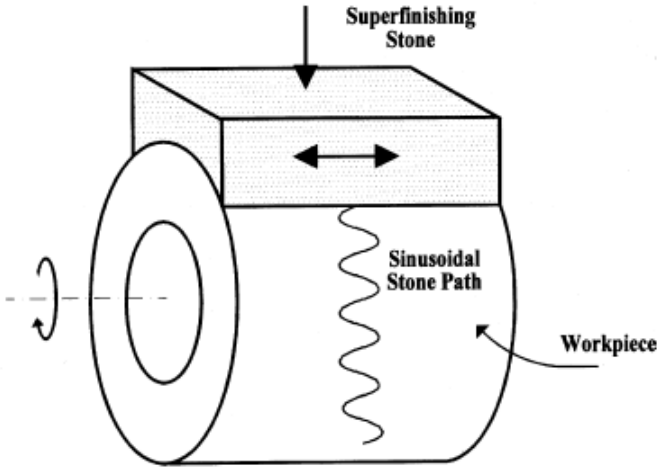

Figure 1.5: Machining configuration of the cylindrical superfinishing process [Chang *et al.*, 2008]

1.2.4 Magnetic Abrasive Finishing (MAF)

Magnetic Abrasive Finishing is one of the advanced finishing process in which a mixture of non-ferromagnetic abrasive particles are mixed with the ferromagnetic iron particles to do the finishing operation through magnetic force. The iron particles hold the abrasives and the accumulated structure thus formed is called the Flexible Magnetic Abrasive Brush (FMAB) and the relative motion between FMAB and the workpiece is responsible for finishing [Kumar *et al.*, 2013]. The magnetic force can be changed by varying the concentration of the magnetic media like pins, flakes or particles. The Figure 1.6 shows the arrangement of the magnetic field for ferromagnetic and non-ferromagnetic workpieces [Hashimoto *et al.*, 2016]

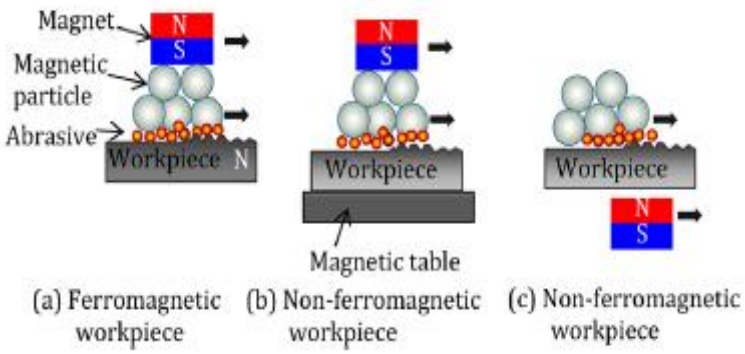

Figure 1.6: Principles of MAF processing [Hashimoto *et al.*, 2016]

It has been proved experimentally that voltage and working gap have significantly effect on the change in surface roughness (ΔR_a) which is followed by abrasive mesh no. and then rotational speed [Singh *et al.*, 2004]. Figure 1.7 shows the schematic arrangement of finishing of external cylindrical surfaces.

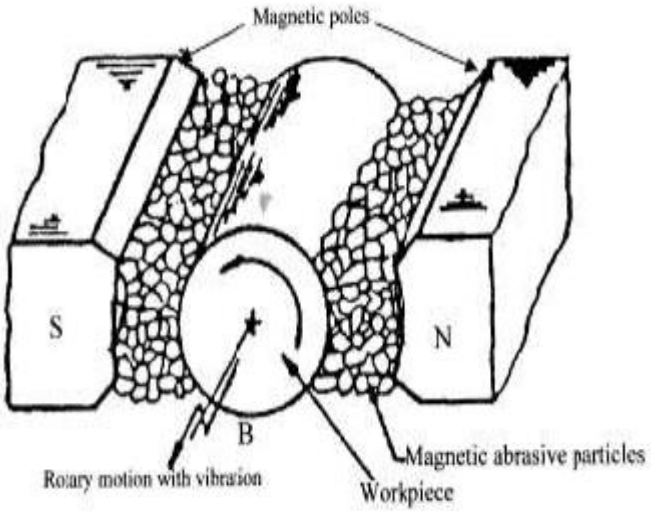

Figure 1.7: Finishing process of cylindrical workpiece in MAF [Kumar *et al.*, 2008]

1.2.5 Magnetorheological Finishing

This process is mainly developed to obtain high precision surface finish in the field of optics but now its application is extended to get the finish in the steel based industries. The main advantage of this process is that one can control the finishing forces involved by just varying the strength of magnetic field. The process uses MR fluid which is a suspension of Carbonyl particles and abrasives in paraffin oil and grease [Fei *et al.*, 2015]. Figure 1.8 shows the magnetorheological effect under the action of magnetic field.

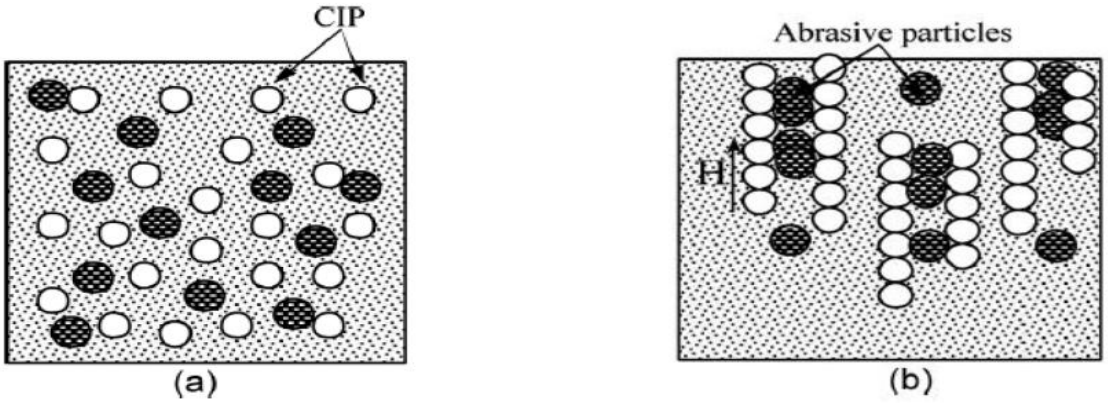

Figure 1.8: Magnetorheological Effect in MR fluid (a) at no magnetic field, and (b) at magnetic field of strength H [Jain, 2008]

In the absence of magnetic field, the fluid is in free flow state but when magnetic field is applied carbonyl particles align themselves in the form of chains and thus hold the abrasives in between them and thus become stiffen [Jain, 2008]. A turning type of apparatus is developed to finish the external cylindrical surfaces such as shafts as shown in the Fig. 1.9.

Due to the rheological properties of MR fluid, this method can be used to finish soft as well as hard materials [Singh *et al.*, 2016].

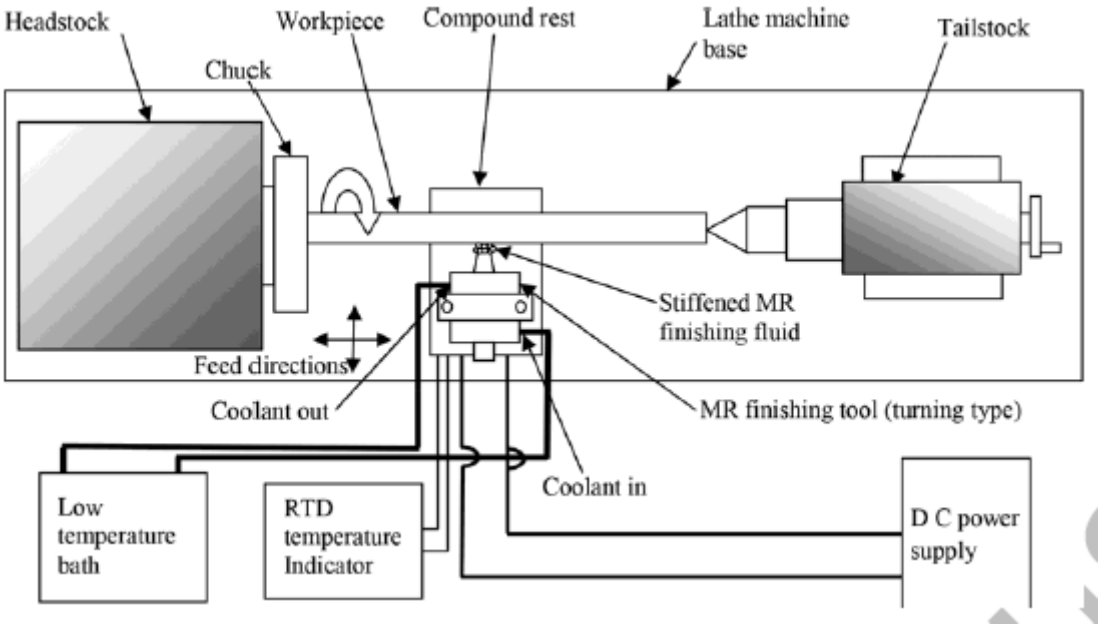

Figure 1.9: A schematic top view of the present new magnetorheological finishing [Singh *et al.*, 2017]

1.3 Applications of C60 steel and the need of nanofinishing

C60 is one of the higher carbon content (about 0.6 %) steels. Due to presence of high carbon content, the machinability of the material is very low. 1060 is the SAE-AISI designation for this material. Mostly this material is used for manufacturing automotive components such as crankshafts, rocker arm shafts, camshafts, rack and pinion steering tie rods, etc.

In automobile sector, the improved surface quality of the product is desired to enhance the wear characteristics and service life of the product. Moreover, the higher quality of the surface is essential to attain the required performance of functions such as fatigue life. Higher fatigue life is required for the power transmitting shafts such as crankshafts. In running condition of the engine, there is very thin oil film present in between the journals on the crankshaft and the loaded portion of the main and the rod bearings. Rough journals result in the sticking of burrs, particles or other debris on the surface of the crankshaft outcomes in the large abrading wear and finally the risk of bearing seizure [www.enginebuildermag.com/1998/09/crankshaft-polishing-make-sure-the-journals-on-the-crankshaft-are-properly-polished/]. The various applications of C60 steel is shown in the Fig. 1.10.

The existing finishing process employed for these automotive components is generally cylindrical grinding. The grinding as stated above results in the involvement of large magnitude of cutting forces which is a cause for not attaining better surface finish value. The limitations associated with the process motivated the author for doing the research regarding finishing process involving small magnitude of cutting forces for precise finishing. Magnetorheological finishing is an ideal process for these requirements as it involves not only small magnitude of cutting forces but also magnetorheological polishing (MRP) fluid has rheological properties which make this process suitable for complex intricate surfaces also.

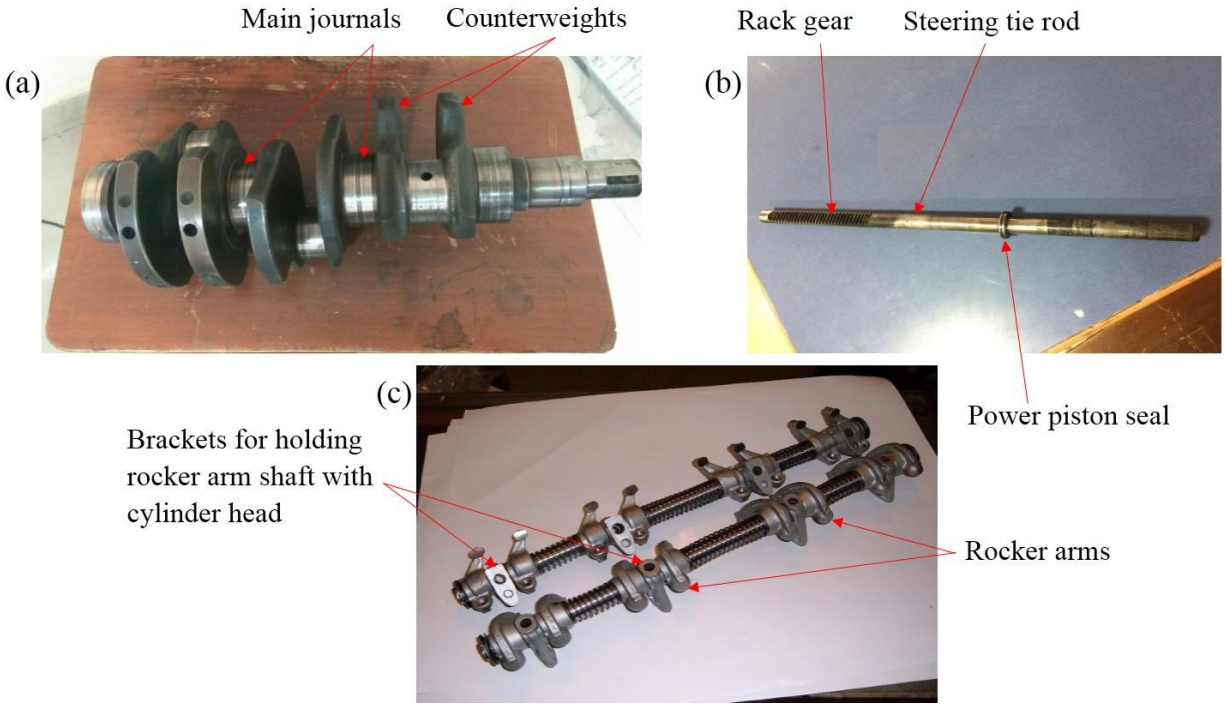

Figure 1.10 Applications of C60 steel (a) crankshaft, (b) rack and pinion steering tie rod, and (c) rocker arm shaft

Chapter 2
Literature Review

2.1 General

In this chapter, the literature of different processes based on the external cylindrical surfaces has been discussed. Also, the experimentation done till now to obtain the effects of different parameters on machining rate and surface roughness value have been reported.

2.2 Review of the literature

Nguyen and Zhang (2011) observed the existence of grinding-hardening in curved surfaces during plunge grinding. To understand the characteristics of grinding hardening, a temperature-dependent finite element heat transfer model comprising a triangular moving heat source was formulated to identify the temperature field. By employing this methodology, the thickness of the grinding-hardened layer was predicted. Steel 1045 was chosen as workpiece and the developed model was verified experimentally. It was observed that the consecutive heating and cooling processes was the main cause of heating cycle in plunge cylindrical grinding, varying from location to location in a workpiece.

Liu *et al*. (2015) discussed the effects of the grinding induced cyclic heating on the properties of the hardened layer in a plunge cylindrical grinding process. The workpiece was chosen as steel EN26. To determine the profile generation of hardened layers, it is necessary to determine the trajectories of grinding induced heat sources which can only be known by knowing the grinding configurations. For example, in a traverse cylindrical grinding, due to simultaneous axial and rotational movements, the hardened layer was found to be non-uniform along the axial direction. While in plunge grinding, the way of work- wheel engagement is important for the uniformity/ continuity of the hardened layer. The main cause of the non-uniformity is the varying depth of cut as shown in the Fig. 2.1(a). To improve this situation, two other efforts are made as shown in the fig. 2.1(b) and 2.1(c) but these also result in the tampering of the hardened layer making its hardness decreased.

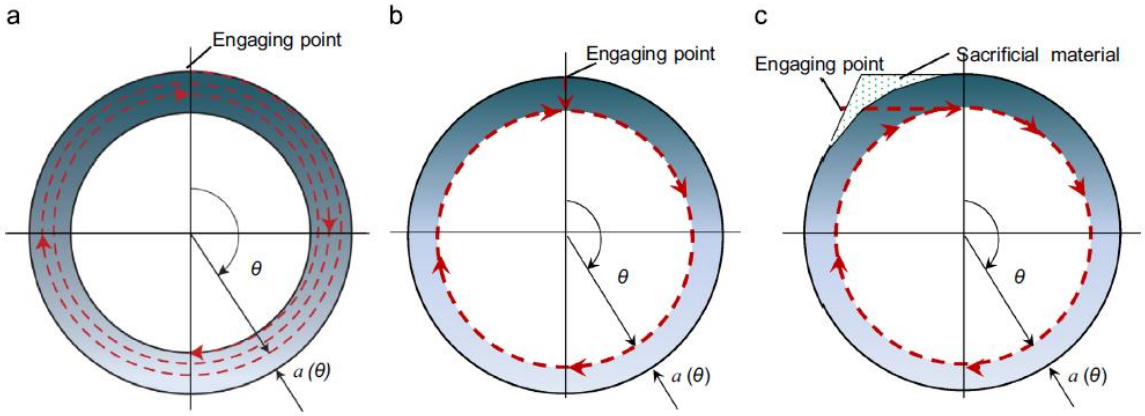

Figure 2.1: Schematics of plunge grinding strategies (a) Spiral grinding, (b) radial grinding, and (c) tangential grinding [Liu *et al.*, 2015]

To overcome the above situation, plunge grinding with multi passes is suggested i.e. removing the required depth of material in multiple revolutions of the workpiece to produce a more uniform and thick hardened layer.

Chang *et al.* (2008) described the experimental investigation of the effect of process parameters on evaluation of superfinished surface texture. Applications of superfinishing include the finishing of bearings, precision automotive components and shafts. A series of time-dependent superfinishing experiments are conducted to study the fundamental characteristics of superfinishing process. The experiment conducted on a case hardened AISI 8119 steel which was mounted on the tailstock of a superfinishing machine with a stone oscillation amplitude of 0.5 mm. The experiments were performed with the different initial average surface roughness and at different workpiece rotation speeds with respect to time as shown in the Fig. 2.2 (a) & (b).

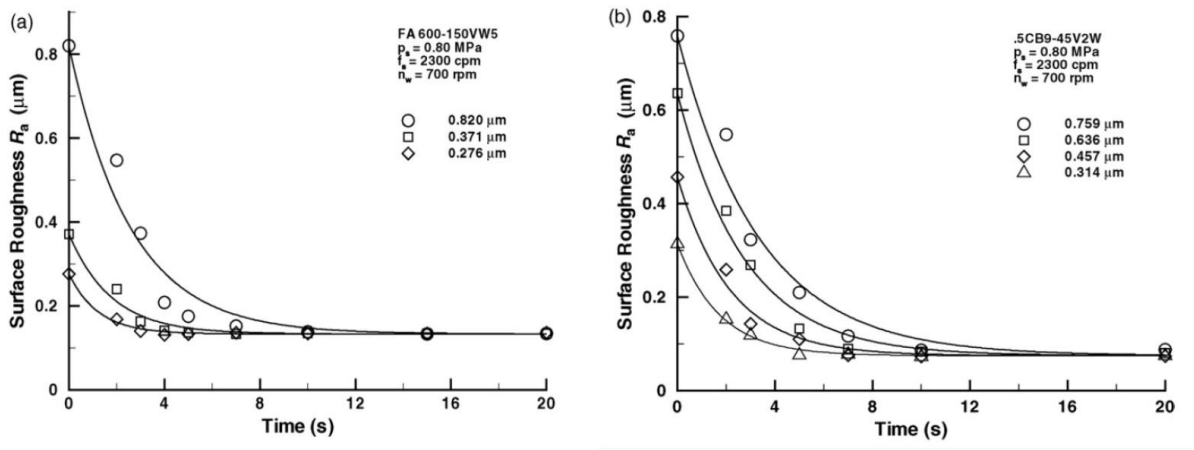

Figure 2.2: Variation in surface roughness, R_a, with machining time (a) at different initial surface roughness, and (b) at different rotational speeds [Chang *et al.*, 2008]

In the end, authors concluded that the superfinished surface has an inherent surface texture with a characteristic surface roughness. The surface texture is shown in the Fig. 2.3 and also the contact pressure has no effect on the transient surface roughness.

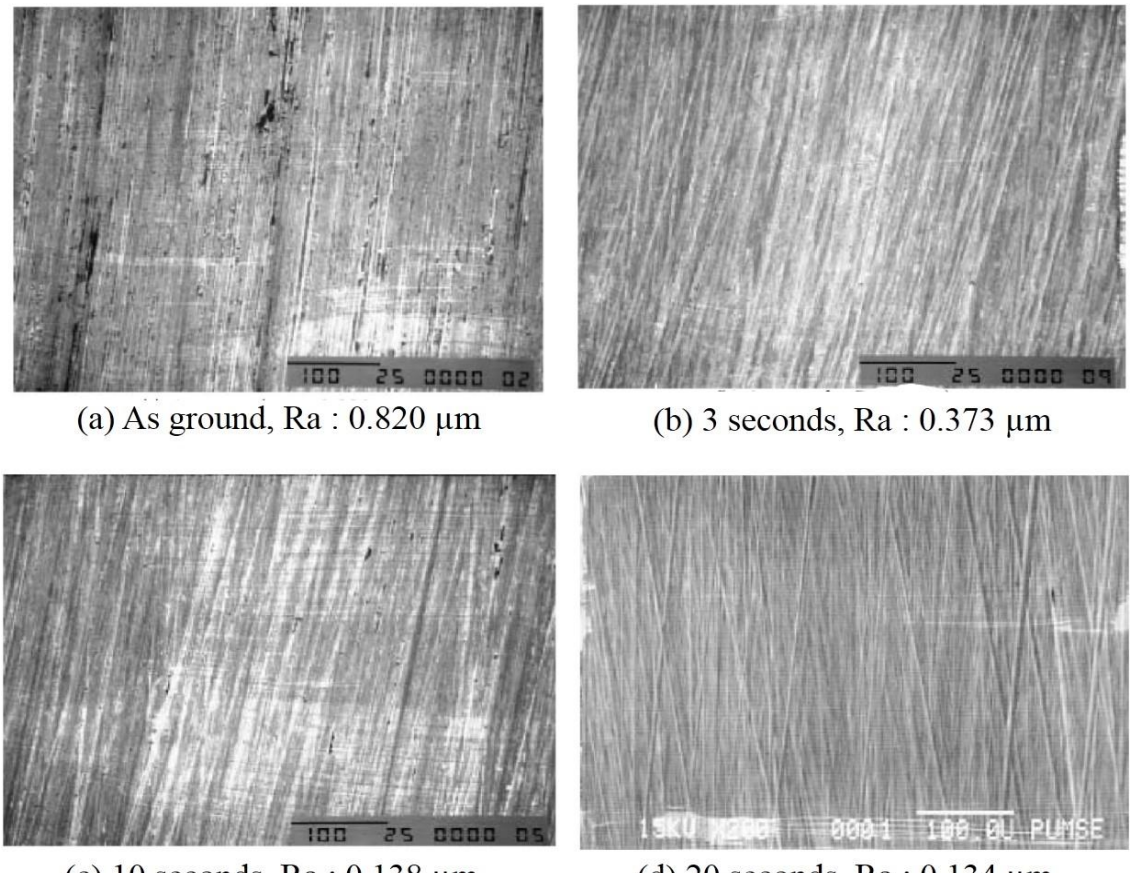

(a) As ground, Ra : 0.820 μm

(b) 3 seconds, Ra : 0.373 μm

(c) 10 seconds, Ra : 0.138 μm

(d) 20 seconds, Ra : 0.134 μm

Figure 2.3: SEM micrographs of the superfinished surface at various process times [Chang *et al.*, 2008]

Hashimoto *et al.* (2016) studied in detail about the processes based on abrasive finishing technology. The authors classified the processes according to the process principles, abrasive states, tools, media, etc. The material removal mechanisms, final finishing range and the specific energies associated with the processes were given along with the assessments of the surfaces created by them. In the end, the authors described the future prospective of the technology.

Singh *et al.* (2011) developed a new precision finishing process for 3D surfaces using ball end MR finishing tool in which specially prepared magnetorheological polishing (MRP) fluid is used as a finishing medium. Experiments were performed on both ferromagnetic (EN31) and non-ferromagnetic (3D copper) workpieces. Working gap is set at 2 mm according to the simulation results and experimentation performed. It was found that with 100 rpm of tool and 100 min of finishing time on ferromagnetic material, the surface roughness decreased from 414.1 nm to 70 nm. With 600 rpm and finishing time of 60 min on non-ferromagnetic material surface roughness decreased from 336.8 nm to 102 nm. Magnetic flux is kept at 0.2T for both the cases. Thus the author proved the capability of the newly developed ball end MR finishing tool to reduce surface roughness and improve the surface characteristics of plane and 3D groove surfaces of ferromagnetic as well as non-ferromagnetic work materials.

Sidpara and Jain (2011) modelled and correlate the normal and tangential forces acting during the magnetorheological fluid based finishing process. A dynamometer is usded to keep online record of the forces acting on the workpiece. The process parameters include volume concentration of CIPs and abrasives, working gap and wheel rotation. Full factorial design was utilized to construct plan of experiments and later on ANOVA is done to quantify the correlation between the forces and process parameters. It was found that the working gap contributed maximum to the forces followed by CIPs concentration while the least contribution was noticed by the wheel speed. It was also found that both the forces increase with increase in CIPs concentration. With increase in wheel speed, normal force increases while the tangential force increases up to a certain limit beyond which it starts decreasing.

Singh *et al.* (2012) studied the effect of finishing time on the surface roughness of fused silica glass using ball end magnetorheological finishing tool. For this experimentation CIPs of CS grade, abrasive powder as cerium oxide and carrier fluid as deionised water are used in 30%, 10% and 60% volume concentration respectively. Finishing cycle time of 30 min was taken, rotation speed at 400 rpm, working gap distance at 1.5 mm, feed rate for two and fro

motion of the workpiece and current supply at 4A and 2.5A was taken into consideration. It was found that the Ra value was decreased from 0.74 nm to 0.14 nm.

Sidpara and Jain (2012) developed a theoretical model of normal and tangential force acting on the workpiece during magnetorheological fluid based finishing (MRFF) process. Normal force was modelled by considering magnetic levitation force while tangential force experienced by the workpiece acted due to the rotation of the carrier wheel. Volume concentration of CIPs, volume concentration of abrasives, working gap and wheel speed were the selected process parameters. In the end authors concluded that normal and tangential force increases with increase in CIPs concentration, however the trend was reversed in case of working gap and abrasive particles concentration.

Jang *et al.* (2012) developed a new set up for deburring using magnetorheological fluid. The authors were successful in applying this process for removal of metal burrs with a height of 200 µm and thickness of 1 µm in micro-moulds with extensive yielding and abrasive wear. The average R_a value of brass decreased from 192 nm to 34 nm after 4 min of processing.

Sidpara and Jain (2013) studied the effects of normal, tangential and axial forces on the curved surface during magnetorheological fluid based finishing process. Angle of curvature of the workpiece, rotational speed of the tool and feed rate are chosen as process parameters. Normal force was found to be more dominant followed by tangential and then axial force. Authors concluded that increasing angle of curvature of the workpiece outcomes in decreasing normal and tangential forces while the rotational speed of the tool and feed rate of the workpiece have an optimum value where the magnitude of these forces are maximum.

Singh *et al.* (2013) mathematically explained the mechanism of material removal in ball end magnetorheological finishing process. The authors prepared a mathematical model for the normal forces generated during the process of finishing. The model was the validiated experimentally by varying the working gap. The authors also explained that with increase in normal force the mechanism changed from three body mechanism to two body wear mechanism as the constraint contact of abrasive particles with the workpiece surface was more in case of higher normal force.

Kordonski *et al.* (2015) observed that that finishing via magnetorheological methods depend upon the stability of the MR fluid which is dependable on the concentration of the magnetic particles and magnetic properties of the particles. Concentration may change due to

evaporation or leakage of the carrier fluid as well as particles sedimentation. Normally the concentration of the particles is the function of viscosity. So the measurement of viscosity is done by the measurement of velocity and pressure difference but since the MR fluid is a non-Newtonian fluid and therefore the viscosity is not only remains function of particle concentration but also shear strain rate. Therefore authors provided 2 novel methods for viscosity measurement. The first one is based on the principle of mutual inductance and second one is based on the changes in the reluctance of MR fluid layer adjacent to the walls.

Liu *et al.* (2015) presented a process to prepare silicone oil based magnetorheological fluids (MRFs) with the addition of nanometer Fe_3O_4 particles. Five different MRF's samples having nanometer Fe_3O_4 particles with mass fractions of 0%, 2%, 4%, 6% and 8% have been prepared. Experiments had been conducted to test the sedimentation stability, zero field viscosity and shear yield stress of these five samples. The results showed that adding a certain amount of nanometer Fe3O4 particles (4% and 6% wt.) into MRFs can improve the performance of MRFs.

Singh *et al.* (2016) made comparison between newly developed magnetorheological finishing tool with flat and curved tool tip surface to perform finishing on external cylindrical surfaces. The mild steel shaft is used as workpiece is used in macroni manufacturing machine. The surface roughness values R_a and Rz were reduced to 54.41% and 40% with flat tip surface and 80.88% and 82.5% with curve tip surface in 90 minutes of finishing time. The experimental process parameters and conditions are given in the Table 2.1. The overall results indicate that the present process with curved tool tip surface is more useful in finishing the external surface of cylindrical workpiece.

Table 2.1: Experimental process parameters and conditions

Parameters	Conditions
Electromagnet magnetizing current	2A
Workpiece rotational speed	443 RPM
Working gap	0.5 mm
SiC abrasives powder	20 volume % of particle size 19 µm
Carbonyl iron powder	20 volume % of particle size 23 µm
Base fluid medium	60 volume % of mineral oil
Workpiece material	Stepped cylindrical mild steel

Maan *et al.* (2016) developed magnetorheological finishing technique for finishing Permanent Mould Punch which is used to manufacture plastic caps. The flat surface is

finished with rotating core ball end tool while the external circular surface is finished by a turning type curved ball end finishing tool. The material of the present permanent mould punch is P20 tool steel with hardness of 431 VHN. Table 2.2 shows the experimental process parameters and conditions. The surface roughness value of flat surface of permanent mould die punch was reduced from 1080 nm to 30 nm in 120 min of finishing using modified ball end with solid rotating tool core. The surface roughness value of external circular of permanent mould die punch was reduced from 630 nm to 80 nm in 120 min of finishing by using turning type magnetorheological finishing process.

Table 2.2: Experimental process parameters and conditions

Parameters	For flat surfaces	For external circular surface
Finishing cycle time	120 min	120 min
Magnetizing current	3A	2A
Rotational speed of tool core	1500 RPM	284 RPM
Working Gap	0.6 mm	0.6 mm
Feed Rate	30 mm/min	50 mm/min

2.3 Research Gaps

From the literature review it is very clear that no work has been done on the finishing of automotive components using magnetorheological fluid based nanofinishing processes. Moreover, there is less work on comparing different finishing processes with magnetorheological fluid based finishing process for external cylindrical surfaces. The detailed research gaps are given below:

- In cylindrical grinding, the heat generated cannot be properly dissipated which results in change of surface properties of the workpiece and a hardened layer is created on the workpiece which is known as grinding-hardening.
- Superfinishing results in inherent surface texture (cross hatch pattern) with a specific surface roughness which remains constant after some time lapse and also the contact pressure acting on the stone has no much significant effect on the final surface finish of the workpiece.
- Also the cutting forces evolved during grinding, lapping, superfinishing and other processes are not controllable which can be possible by using magnetic assisted finishing processes.

- Surface roughness value is lowest for magnetorheological finishing (MRF) method as compared to other finishing methods and can be used for all the materials whether it is hard or soft as MR fluid used in it has got rheological properties.
- Till now, the relative motion between the workpiece and tool is introduced by giving rotation to either one of them.
- There is no feeding arrangement used till now along the axis of the cylindrical workpiece so that an automatic process can be accomplished.

2.4 Objectives of the Present Work

Magnetorheological finishing can be an affirmative candidate in finishing external cylindrical surfaces over other finishing processes to meet today's industries requirements which include mirror finish precision components like plungers and various gauges for calibration. Therefore, an attempt can be made to make modifications in the already existing set up to get better surface finish in lowest possible time. Also the developed modified set up can be utilized to finish industrial based applications. Following are the objectives of the present work:

- To make modifications in the magnetorheological finishing (MRF) tool to achieve better surface finish like simultaneously rotating workpiece and tool and look its effect on the surface finish in various time dependent trials. Also, to provide feed rate for linear movement on tool.
- To demonstrate the capability of the modified rotating core based magnetorheological finishing process in finishing of hard materials such as steel of grade C60 used in manufacturing of automotive components such as crankshafts, rocker arm shafts, rack and pinion steering tie rods, etc.
- To optimize the process parameters for finishing of steel of grade C60 using present magnetorheological finishing process.

2.5 Material Selection

The material used for manufacturing of automotive shaft components such as crankshafts, rocker arm shafts, rack and pinion steering tie rod is very hard and tough. Thus it has low machinability. Moreover these components require high fatigue strength as they are subjected

to cyclic loads. Spectroscopy test revealed the grade of material as steel of grade C60 along with its detailed chemical composition which is shown in the Table 2.3.

Table 2.3: Chemical composition of C60 steel

Constituting elements	C	Si	Mn	P	S	Cr	Mo	Ni	Fe
Mass percentage	0.583	0.311	0.831	0.026	0.034	0.197	0.016	0.036	Balance

Figure 2.4 shows the shafts of C60 steel used for experimentation and parametric analysis. The effect of heat treatment processes on C60 grade is studied by various researchers. [Abrao *et al.,* 2014] studied the effects of different heat treatment processes namely subcritical annealing, full annealing and hardening through quenching and tempering. The samples are then deep rolled with different rolling pressure and number of passes. Micro hardness, surface hardness, tensile strength, residual stress and subsurface microhardness of the samples are analysed. Authors concluded that workpiece with full annealing face more severity to the plastic deformation while on the other hand hardening samples show no signs of deformation. The higher the hardness of the workpiece material the lesser is the effect of deep rolling on it.

Figure 2.4: Grounded shafts of steel of grade C60 used for experimentation

The properties of C60 or AISI 1060 steel are listed in the Table 2.4.

Table 2.4: Properties of C60 or AISI 1060 steel

Property	Values
Tensile Strength	850 – 1000 MPa
Hardness	~250 HB
Ferromagnetic	Yes

2.6 Methodology

The major objective of this work is to make modifications in existing process to get an improved process with the better capabilities and also demonstrate this process in finishing of C60 steel which has major applications in the automobile industries. Step by step procedures have been followed to get the required objectives accomplished. Figure 2.4 shows the methodology in the form of a flow chart.

1) Dedicated literature survey regarding different finishing processes for external cylindrical surfaces, the type of material used, range of final surface finish value obtained and comparison of other finishing processes with the magnetic assisted finishing processes.

2) Modifications are made in the existing magnetorheological finishing process to get an improved process with provision of giving rotation to both the tool and workpiece simultaneously. Moreover feed rate is provided to the tool to fully automate the process.

3) Preliminary experimentation is done with the modified process to demonstrate the capabilities of modified improved process.

4) Applications related to automobile industry has been selected for finishing. Spectroscopy test revealed the presence of steel of grade C60. Moreover there is very less work on this steel grade according to the studied literature review.

5) Those parameters which are significantly effecting the process in preliminary experimentation are selected for further analysis.

6) Design of experiments are created using the Design of Experts v6 Software.

7) Experimentation is performed according to the plan of experiments made by the software.

8) Conclusion is given regarding the effect of parameters and their interaction on the response variable.

9) Finally the parameters are optimized to obtain the best value of the response variable.

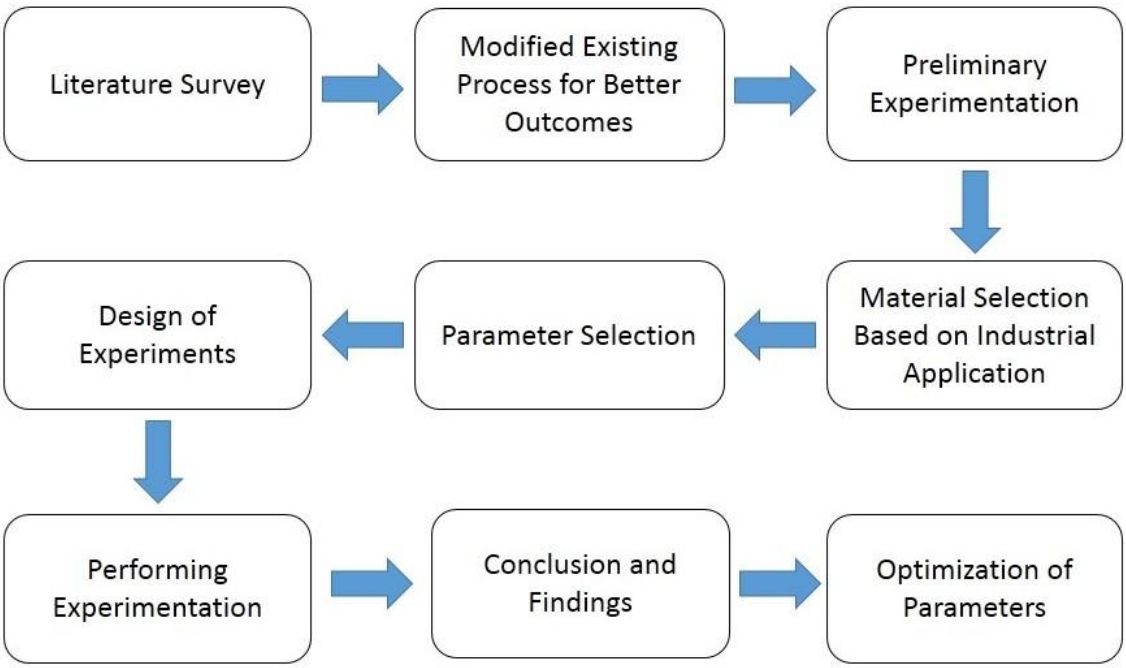

Figure 2.5: Flow chart of the methodology being followed in present research work

Chapter 3
Preliminary Experimentation to Examine the Process Performance

3.1 Introduction

This chapter explained the preliminary experimentation and mechanism of the process involved. The preliminary experimentation is done on the mild steel cylindrical shaft which has its application in macroni making machine. A temporary setup is designed to give simultaneously rotation to the workpiece and tool core. The detailed experimentation setup and the mechanism involved are formulated in the later on discussed sections.

3.2 Preliminary Experimentation

Experimentation was performed on the external surface of the mild steel stepped cylindrical workpiece. The composition of the material included Fe 98.2%, C 0.273%, Si 0.217%, Mn 0.577%, P 0.0421%, S 0.0743%, Cr 0.124%, Mo 0.01%, Ni 0.14%, Al 0.0137%, Co 0.01%, Cu 0.18%, Nb 0.005%, Ti 0.023%, V 0.0188%, W 0.025%, and Pb 0.05%. Stepped mild steel cylindrical shaft which act as workpiece was used in macaroni machine. To provide smooth and noiseless operation by reducing the friction and wear of the cylindrical shaft, fine finishing is needed on the outer surface of the shaft. The experimentation utilized magnetorhelogical process with stationary curved tool tip and rotating flat tool tip as shown in the Figs. 3.1 (a) and (b).

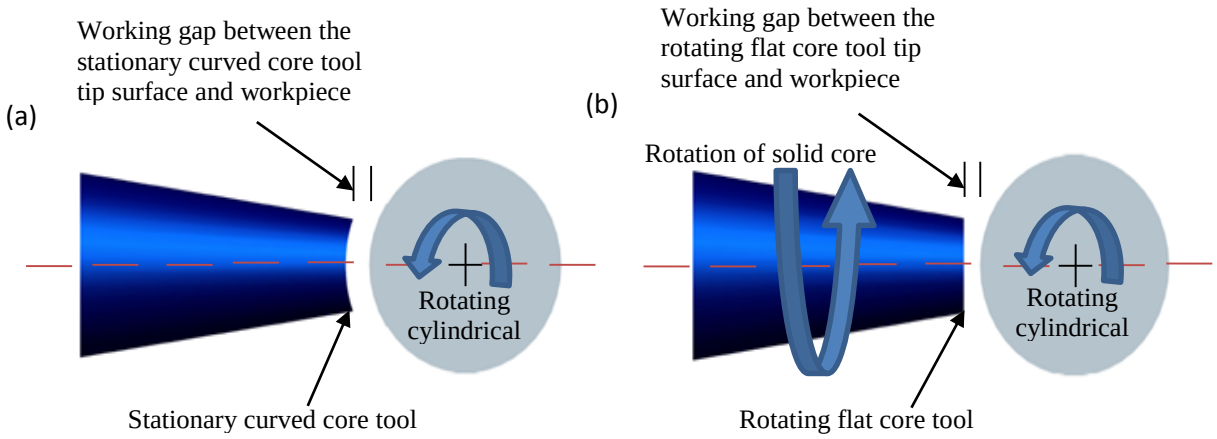

Figure 3.1: Enlarged view of working gap with (a) stationary curved core tool tip surface, and (b) a rotating flat core tool tip surface

The two electromagnetic tools one with stationary curved tool tip and the other with rotating flat tool tip are horizontally stalled on the programmable z slide of the experimental set up. The setup is PLC (Programmable Logic Controller) controlled with the help of servo drives and motors. This helped to provide very precise control on the feed and speed of the tool and cylindrical workpiece. The complete experimentation is done in two phases. In the first phase, the electromagnetic stationary curved tool tip is used while in the second phase the electromagnetic rotating flat tool tip is used. The programmable servo motor give rotary motion to the flat tool tip while the curved tool tip is kept stationary. Another programmable servo motor transmit reciprocating motion to the tool mounted on the horizontal z slide for feeding purpose in both the phases. The cylindrical workpiece is held between the two supports with the ball bearings and is rotated by a separate programmable servo motor through the belt pulley drive. The whole arrangement is placed on the non-magnetic breadboard. The top view of the actual experimental setup is shown in the Figs. 3.2 (a) and (b).

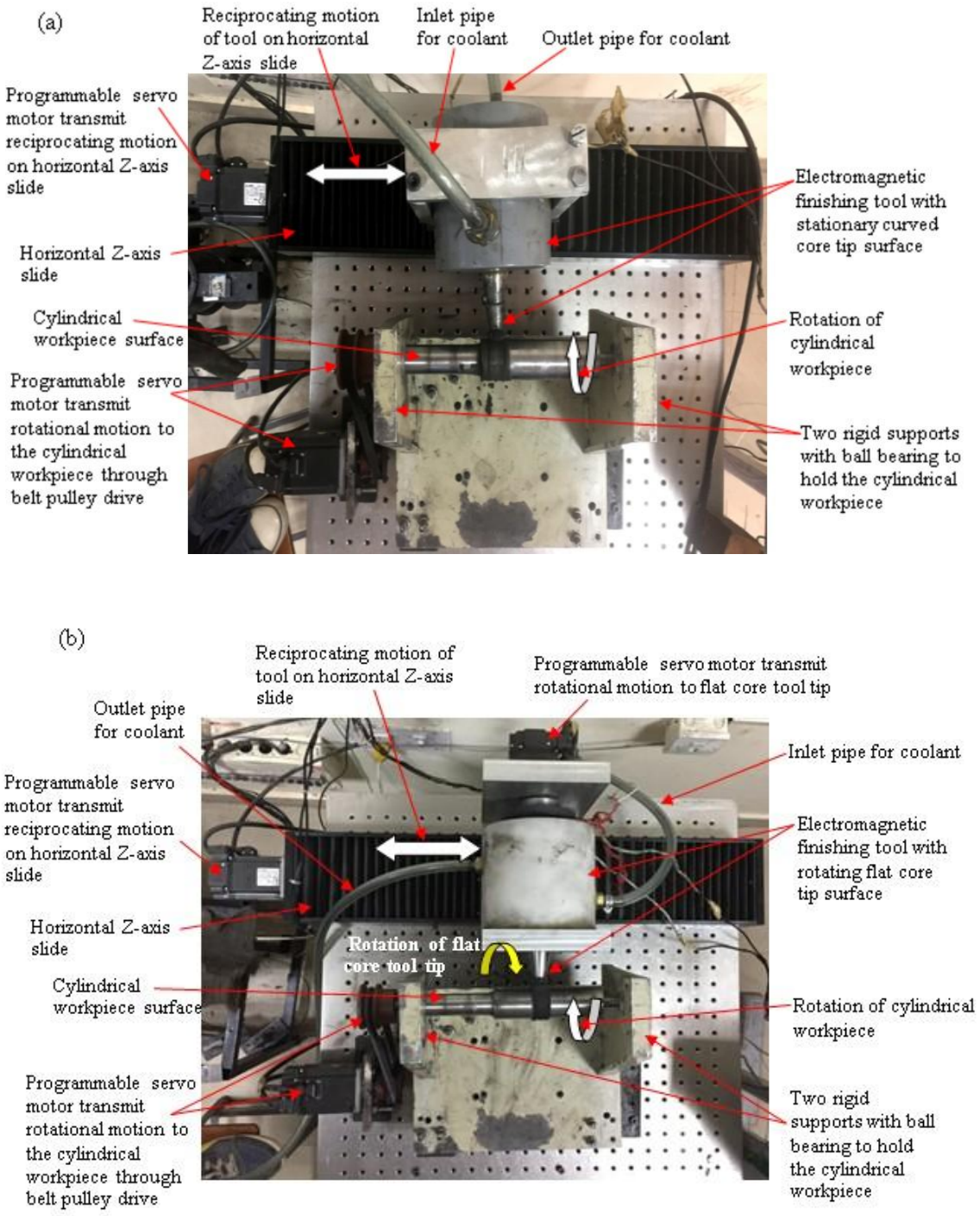

Figure 3.2: Top view of the magnetorheological finishing process (a) with a stationary curved core tool tip surface, and (b) with a rotating flat core tool tip surface

Both electromagnetic tools were cooled with the help of transformer oil circulation throughout the electromagnetic coils. Oil cooling was done by the help of refrigeration system. In the previous work the experimentation was done on solid core flat and curved tool tips and both the tools were kept stationary [Singh *et al.*, 2016]. But in recent experimentation the rotation was provided to the flat tool tip while the curved tool tip remained stationary.

The experimentation was done with both types of tools. The MR polishing fluid was applied on the tip of both the tools before performing experiments. The composition of the MR polishing fluid was taken as 60% of the carrier fluid (paraffin oil 80% and AP3 grease 20% by weight), 20% of the abrasive particles of 600 mesh size and 20% of the carbonyl iron particles (CIPs) of 400 mesh size by volume. The MR polishing fluid got strengthened by the magnetic field produced due to the magnetizing d.c. current. The stiffened chains of CIPs hold the active abrasive particles tightly and material gets removed from the surface of the workpiece by its relative movement.

Higher material removal rate was noted in the rotary flat tool tip because of the kinetic energy of the abrasives which help to remove the material in excessive rate. Both the tools were provided with the same feed rate of 30 mm/min. During trials, various combinations of rotational speeds of the workpiece and the tool core were made and their effect on the material removal rate in terms of surface roughness value was observed. It had been observed that lower rotational speed of workpiece and higher rotational speed of the tool core results in significant material removal and thus the rotational speeds of the workpiece and the tool core are taken as 100 rpm and 500 rpm, respectively. The electromagnetic MR finishing tools used in both the phases of experiments had 2200 number of turns of copper wire (i.e. 20 standard wire gauge). Since the number of turns and the current in the electromagnetic coil directly impact the magnetic flux. Therefore to generate the same magnetic fluxes in both the cases, same value of current is applied using a d.c. regulated supply. The experimentation was done on the stepped cylindrical mild steel workpiece to examine the finishing time and its effect on the surface roughness values by using the stationary curved tool tip and rotating flat tool tip. Roughness values were measured by Mitutoyo surftest SJ-400 with the cut off length of 0.25 mm. The parameters and conditions based on the preliminary experiments are given in the Table 3.1. These parameters and conditions are employed to finish the present cylindrical shaft workpiece for both the finishing cases. The main purpose of the recent work is to compare the finishing performance of improved finishing process using rotating flat tool tip with the stationary curved tool tip by keeping other parameters and conditions same. Moreover the material removal mechanism for improved finishing process is also studied.

Table 3.1: Experimental processes parameters and conditions

Parameters	Stationary curved core electromagnetic tool tip	Rotating flat core electromagnetic tool tip
Magnetizing current	2A	2A
Working gap	0.6mm	0.6mm
Feed rate	30mm/min	30mm/min
Rotational speed of cylindrical workpiece	100rpm	100rpm
Rotational speed of core tool tip	----	500rpm
Finishing length on workpiece	20mm	20mm
Each finishing cycle time	30min	30min
Total finishing cycle time	90 min	90 min

3.3 Mechanism of the process

The detailed mechanism of material removal in the rotating flat core tool tip can be understood in three stages as shown in Fig. 3.3.

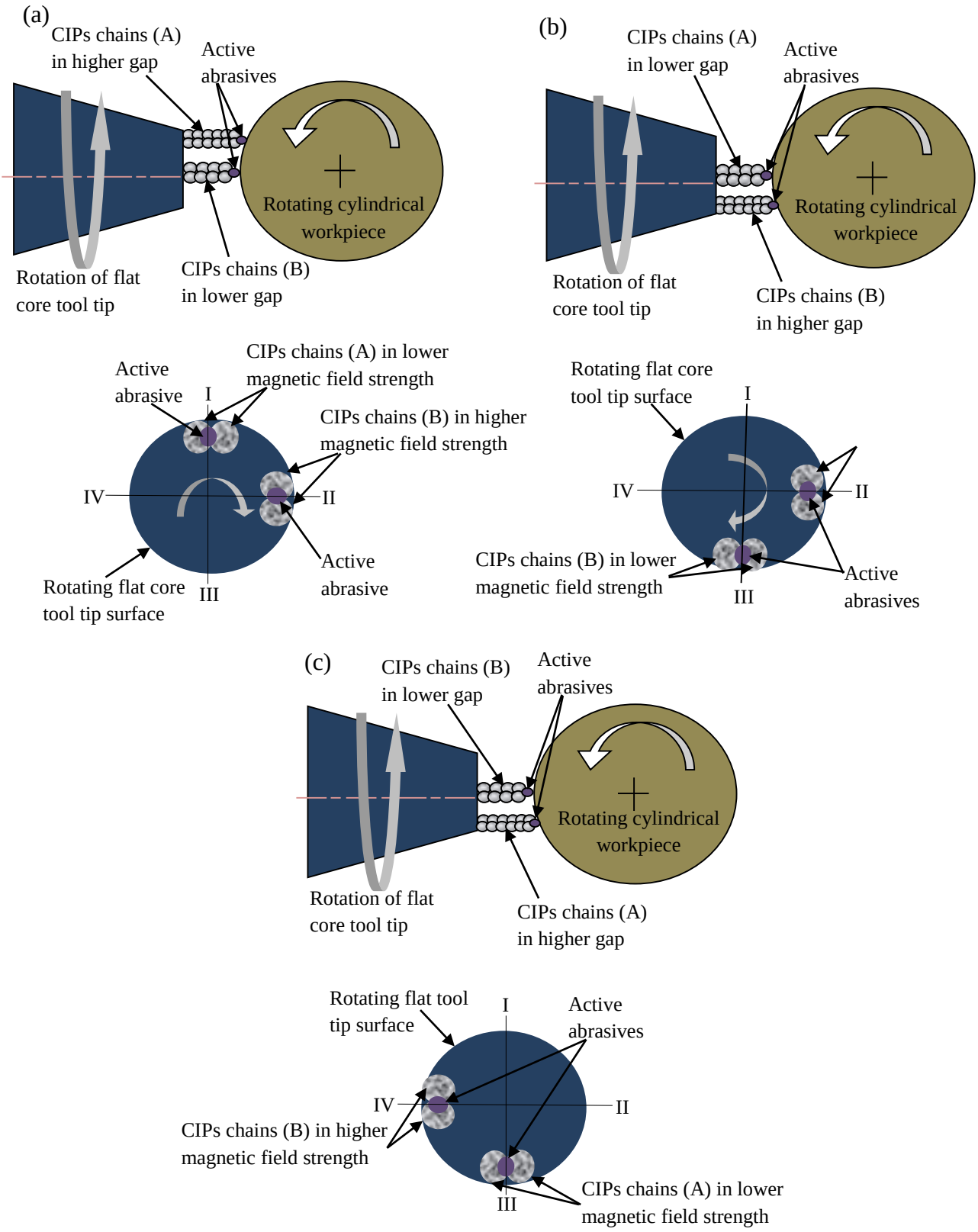

Figure 3.3: Schematic representation of a rotation of active abrasive with CIPs chains during rotation of flat core tool tip surface (also view from right hand side) in high and low magnetic field strengths (a) at any instant, (b) after 90^0 rotation and (c) after 180^0 rotation

Let the surface of the flat core tool tip is divided into the four portions i.e. I, II, III and IV. Consider the two CIPs chains A and B is located at I and II in a particular instant. Due to the cylindrical outer surface, the working gap between the rotating flat core tool tip surface and outer surface of the cylindrical workpiece is varied across the flat core tool tip surface. The strength of the magnetic field is less where the gap between the external surface of cylindrical workpiece and the rotating core tool tip surface is more [Maan *et al.,* 2017] and vice versa. As shown in the Fig. 3.3(a), the gap is more at the location I where the CIPs chains (A) are presented and gap is less at the location II where CIPs chains (B) is presented. This means that magnetic field strength is lesser at location I as compared to the location II. This indicates that the active abrasive held by the CIPs chains (A) is comparatively loosely gripped and the active abrasive held by the CIPs chains (B) is comparatively strongly gripped. Now, when the flat core tool tip surface rotates which result in the rotation of the CIPs chains also along with it. After 90^0 rotation of the flat core tool tip surface from the location I, the CIPs chains (A) moves to the location II and the CIPs chains (B) moves to the location III as shown in the Fig. 3.3(b). The loose gripping of the active abrasive by the CIPs chains (A) at the location I results in changing orientation of the cutting edges of the active abrasive during its travel from location I to location II. When active abrasive comes to location II, a new cutting edge of the same active abrasive comes in contact with the cylindrical workpiece surface. Further, location II has lesser gap and it has high magnetic field strength. Thus, active abrasive strongly gripped with CIPs chains (A) performs finishing operation at this location with the new cutting edge. At the same time CIPs chains (B) is at location III where again gap is more and comparatively there is lesser magnetic field strength. This results in the lesser gripping of the active abrasive with CIPs chains (B). After 180^0 rotation of the flat core tool tip surface from the location I, the CIPs chains (A) moves to the location III and the CIPs chains (B) moves to the location IV as shown in the Fig. 3.3(c). During the travel of CIPs chains (B) from the location III to IV, the orientation of the cutting edges of the loosely bond active abrasive held by the CIPs chains (B) changes. Thus, at location IV, a new cutting edge of the active abrasive with strongly gripped by the CIPs chains (B) is available for performing the finishing operation where gap is less. At the same time, CIPs chains (A) after finishing at the location II moves to the location III where gap is more. Thus, this cycle is repeated continuously with the rotation of flat core tool tip surface. The active abrasive with CIPs chains are continuously changed the orientation of cutting

edges from the lower to higher magnetic field strength region and vice-versa. Also, the significant material removal can take place at locations II and IV because of low gap and high magnetic field strength. But, at locations I and III, the orientation of the cutting edges of the loosely bond active abrasive held by the CIPs chains changes because of higher gap and low magnetic field strength. Thus, on every rotation of the flat core tool tip surface, a different cutting edge of active abrasive with CIPs chains passes through locations I and III and available with greater strength at locations II and IV for performing the finishing on external surface of the cylindrical workpiece.

3.4 Results and Discussion

The effect of change in average surface roughness value R_a at different MR finishing cycle time using stationary curved core tool tip and rotating flat core tool tip on outer surface of cylindrical workpiece with their corresponding percentage variation is reported in Table 3.2. Using MR finishing process with stationary curved core tool tip, the average surface roughness value R_a is cut down from the initial value of 740 nm to 450 nm in first 30 minutes, 450 nm to 290 nm in second next 30 minutes and 290 nm to 210 nm in third next 30 minutes of finishing cycle. When MR finishing process with a rotating flat core tool tip is used, the average roughness value R_a is reduced from the initial value of 740 nm to 250 nm in first 30 minutes, 250 nm to 90 nm in second next 30 minutes and 90 nm to 40 nm in third next 30 minutes of finishing cycle.

Table 3.2: Effect of the change in surface roughness values at different finishing time during MR finishing on the external surface of stepped cylindrical mild steel workpiece using the stationary curved core tool tip and rotating flat core tool tip

Working cycle time (min)	Stationary curved core tool tip		Rotating flat core tool tip	
	External cylindrical surface roughness (nm)	% change in roughness	External cylindrical surface roughness (nm)	% change in roughness
0	740	-	740	-
30	450	39.18	250	66.2
60	290	35.55	90	64
90	210	27.58	40	55.55

Also, it can be noticed from the Table 3.2 that the R_a value obtained after first 30 minutes of the experiment with rotating flat core tool tip is even less than the R_a value

obtained after first 60 minutes of the experiment with stationary curved core tool tip. This proves the effectiveness of newly developed process with respect to finishing time. Also, there is comparatively more decrease in percentage variation in R_a values on moving from first to last 30 minutes of experimentation. This is due to the fact that roughness peaks has the lowest base area at their uppermost portion and thus less force is required to overcome the shear strength of the cylindrical workpiece material. As finishing cycle time increases, the base area of the roughness peaks starts increasing and thus larger force is required to overcome the shear strength. That is why the percentage variation in R_a values starts decreasing in subsequent 30 minutes of experimentation.

The surface roughness profiles of initial and final cylindrical external surface after 90 minutes of MR finishing operation using stationary curved core tool tip and rotating flat core tool tip are shown in the Figs. 3.4 (a), (b) and (c) respectively.

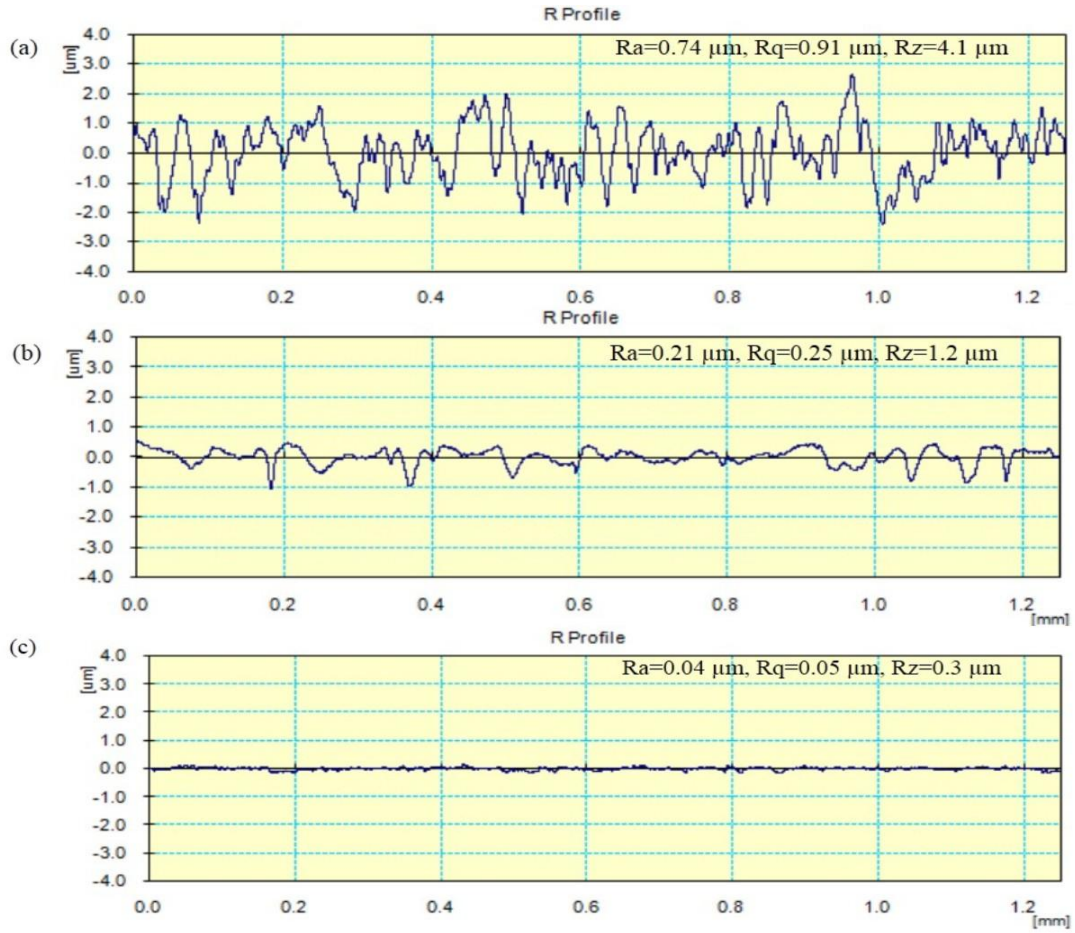

Figure 3.4: Surface roughness profiles of external cylindrical mild steel workpiece, (a) initial ground surface, (b) after 90 min of MR finishing with stationary curved core tool tip and (c) after 90 min of MR finishing with rotating flat core tool tip

The scanning electron microscope (SEM) photographs at 1000x optical zoom of the initial surface roughness and after 90 minutes of MR finishing with the stationary curved core tool tip and the rotating flat core tool tip with the same experimental parameters and conditions are shown in the Fig. 3.5(a), (b) and (c) respectively. Before finishing, the external cylindrical surface showed scratches and marks (Fig. 3.5(a)). After 90 minutes of MR finishing using stationary curved core tool tip, there is lesser enhancement in the surface quality of the external cylindrical surface (Fig. 3.5(b)) as compared to the rotating flat core tool tip (Fig. 3.5(c)). A mirror image test was also conducted as shown in the Fig. 3.5(d). The mirror image test showed the better surface characteristics obtained while using the rotating flat core tool tip as compared to stationary curved core tool tip after 90 minutes of MR finishing.

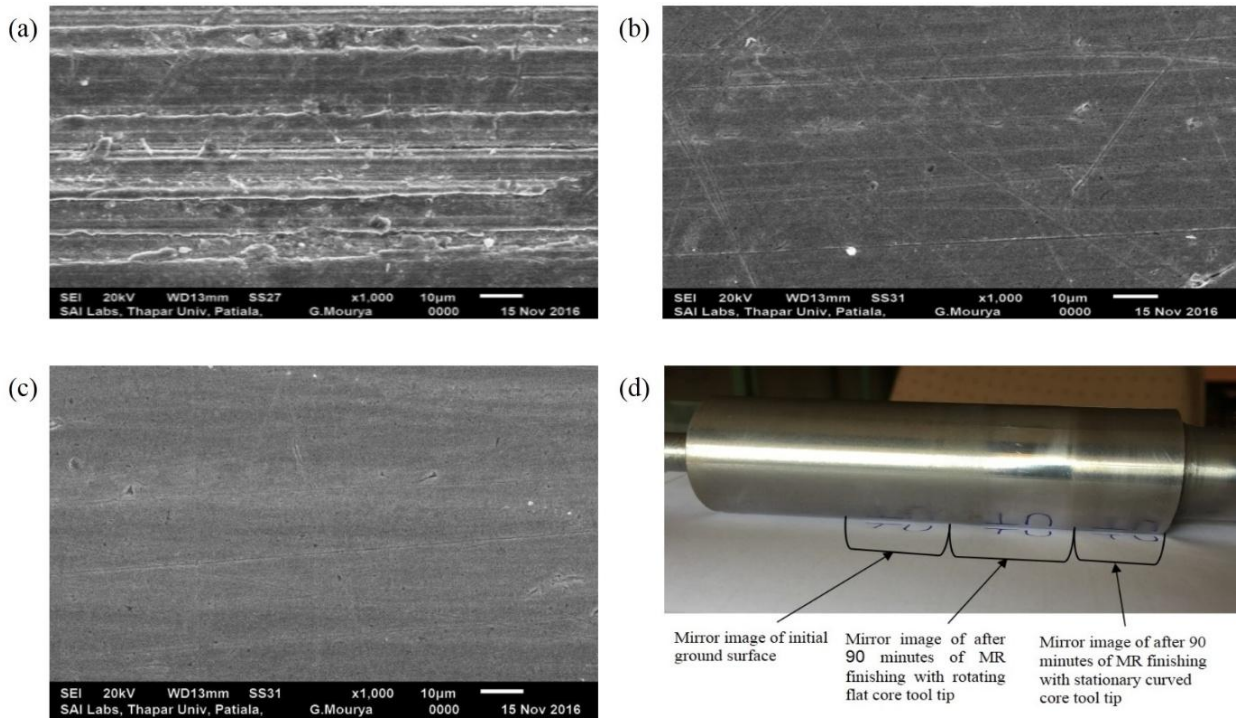

Figure 3.5: Scanning electron microscope (SEM) photographs at 1000x of external surface of cylindrical mild steel workpiece (a) initial ground surface, (b) after 90 minutes of MR finishing with stationary curved core tool tip, (c) after 90 minutes of MR finishing with rotating flat core tool tip and (d) mirror images of initial ground surface, and after 90 minutes of MR finishing with the rotating flat core tool tip and stationary curved core tool tip

It is depicted from the SEM and mirror image analysis that there is great improvement in finishing outer surface of the cylindrical mild steel workpiece using a rotating flat core tool

tip than the stationary curved core tool tip with same experimental parameters and conditions. Hence, the present developed improved magnetorheological finishing method with the rotating flat core tool tip is found more effective process for finishing the external cylindrical surfaces than the stationary curved core tool tip. Moreover, the present developed process is more useful in nano level finishing of automotive transmission parts such as armature shaft, stepped shaft, turbo charger shaft, gear pump shaft, piston pins, piston rods, hydraulic pump pistons, brake pistons, vacuum pistons, rotogravure cylinder, steering rack bar, transmission yoke and shafts used in gear etc.

3.5 Conclusions

From the results, following conclusions can be drawn.

- Kinetic energy of the abrasive particles with rotation of a flat core tool tip has a significantly effect on the material removal rate and better finishing performance.
- Due to the rotation of a flat core tool tip, the CIPs chains get transferred from the lower magnetic field strength to higher magnetic field strength in the working gap which results in changing orientation of the active abrasives and new cutting edges are available for finishing operation instead of same cutting edges as in stationary curved core tool tip.
- R_a value is reduced from 740 nm to 210 nm in 90 minutes of MR finishing with the stationary curved core tool tip,
- R_a value is reduced from 740 nm to 40 nm in 90 minutes of MR finishing with the rotating flat core tool tip.
- Scanning electron microscope (SEM) photographs and mirror images have verified the major enhancement in surface characteristics with the rotating flat core tool tip as compared to the stationary curved core tool tip.

Chapter 4
Parametric Analysis for Finishing of External Cylindrical Surface of C60 Steel

4.1 Introduction

The modified rotating core based magnetorheological finishing process was used for the detailed study of finishing process using different parameters on steel of grade C60 (ferromagnetic). The study was conducted using statistical design of experiments employing Central Composite Design (CCD) approach. Based on the trials and preliminary experimentation, four parameters i.e. current, tool rotation, workpiece rotation and abrasives concentration were chosen. Since the initial surface roughness value is different for different workpiece samples, therefore the percentage reduction in surface roughness (%ΔRa) is taken as response value. To analyse the effect of these parameters on the response value, response surface methodology (RSM) had been employed. The experimental outcomes were discussed and the finishing parameters were optimized to obtain the best finishing results. Analysis of the experimental data showed that the supplied current and tool rotational were mainly contributing to the value of response variable i.e. percentage reduction in surface roughness ($\%\Delta R_a$). This confirmed the significant role of tool rotation in present developed process for the excessive finishing performance which was not there in the existing nanofinishing process. The surface finish was obtained as low as 52 nm from the initial value of about 350 nm in 30 minutes of finishing time. In order to study the finished surface morphology, scanning electron microscope was also conducted.

4.2 Process Parameters

Based on the literature survey and preliminary experimentation, it was found that the four independent controllable parameters namely current, tool rotation, workpiece rotation and abrasive concentration had a significant effect on the finishing of various materials. These parameters are explained in detail as given below:

4.2.1 Current (I)

The current is supplied to the electromagnetic coil using a DC regulated power supply. The supplied current induced a magnetic field in the form of concentric closed loops. The magnetic field strength (H) is replaced with the magnetic flux density (B) as the later is comparatively easily measurable according to Eq. (4.1).

$$B = \mu_0 H \tag{4.1}$$

Where, μ_0 is the permeability of free space

The strength of magnetic flux density which in turn depends on the supply of the magnetizing current has significant influence on the rheological properties of the MRP fluid that is applied at the tip surface of the tool. By varying the magnitude of magnetizing current, the stiffness of the MRP fluid can be controlled. Also indentation force is dependent on the magnetizing current. Experiments were conducted by varying the magnetizing current from 1.5 to 3.5 A. These values of current were selected in the range on the basis of preliminary experimentation and the prescribed design of the electromagnet.

4.2.2 Tool Rotation (T)

The rotation of the tool core has significant influence on the finishing performance. The rotation of the tool provides necessary tangential force which helps in shearing off roughness peaks in the form of micro chips during finishing. It is observed from the preliminary experiments that higher tool rotation gives better finishing but too high value outcomes in scattering of MRP fluid in gap between the workpiece and tool as large centrifugal force comes into action. Experimental range for the tool rotation was selected as 1200 rpm to 2200 rpm.

4.2.3 Workpiece rotation (W)

The primary purpose of the workpiece rotation is to uniformly finish the entire external circumferential surface of the cylindrical workpiece instead of a particular finishing spot. Workpiece rotational speed provide the required relative motion to the process. Relative motion results in effective material removal. However a high workpiece rotation has adverse effect on the material removal rate which will be discussed in detail later on. Thus the

experiments were conducted in the range of 60 rpm to 140 rpm based on the preliminary experimentation.

4.2.4 Abrasives Concentration (A)

Abrasive particles are added in the MR fluid in order to remove the material in the form of micro chips. The chipping off action is performed by the active abrasive particles which comes in contact with the workpiece surface. These abrasive particles are gripped between the CIPs chains. In the presence of magnetic field produced by the electromagnetic tool, the CIPs chains get attracted towards the tool and the abrasive particles due to its diamagnetic nature shifts from the higher magnetic field to lower magnetic field and thus indent into the roughness peaks of the workpiece surface due to magnetic levitation force. Experiments were conducted with the volume concentration in percentage varying from 10% to 30%, as per the design levels.

4.3 Design of Experiments

Response surface methodology (RSM) is an aggregation of statistical and mathematical methods that are useful for modeling and analyzing engineering problems. RSM also quantifies the relationship between the controllable input parameters and the obtained response surfaces. Design of experiments (DOE) is an important aspect of RSM. The purpose of DOE is to choose the points where the value of the response should be determined. There are different methodologies available for the construction of design of experiments. To know the interaction between the different independent controllable variables, a second order model is employed which can be best constructed by the Central Composite Design (CCD) methodology. The plan of experiments of the present research is shown in the Table 4.1. To know the individual and the combined influence of the controllable process variables on the response, ‘F’ test from the analysis of variance (ANOVA) was conducted. In the present work, the MR polishing fluid constitutes 60% of the carrier fluid (paraffin oil 80% and AP3 grease 20% by weight), 20% of the abrasive particles of 600 mesh size and 20% of the carbonyl iron particles (CIPs) of 400 mesh size by volume.

Table 4.1: Independent controllable variables and their corresponding coded levels

S. No.	Parameter	Unit	Levels				
			-2	-1	0	1	2
1	Current (I)	A	1.5	2	2.5	3	3.5
2	Tool rotation (T)	r/min	1200	1450	1700	1950	2200
3	Workpiece rotation (W)	r/min	60	80	100	120	140
4	Abrasives concentration (A)	%	10	15	20	25	30

Table 4.2: Experimental conditions

Parameters	Conditions
Finishing cycle time	30 min
Abrasives silicon carbide (SiC) powder	600 mesh
Constant feed rate to workpiece for to and fro motion	30 mm/min
Workpiece material	C60 (ferromagnetic)
CIP powder	400 mesh

The experimental parameters and conditions are presented in the Table 4.2. The finishing cycle time to perform each trial was taken as 30 minutes. Silicon carbide (SiC) abrasives of 600 mesh size was taken and feed rate of 30 mm/min had been provided. Ferromagnetic workpiece material of steel of grade C60 was chosen as workpiece which had its applications in manufacturing of crank shafts, rocker arm shafts, steering tie rods, etc. The mesh size of powder of carbonyl iron particles (CIPs) was taken. The plan of experiments to perform parametric analysis is presented in the Table 4.3. As depicted from the table, out of certain independent controllable parameters, four were selected namely current (I), tool rotation (T), workpiece rotation (W) and abrasives concentration (A).

Table 4.3: Plan of experiments

Run order	Std order	Actual Values			
		Current (I)	Tool Rotation (T)	W/p Rotation (W)	Abrasives concentration (A)
25	1	2.5	1700	100	20
29	2	2.5	1700	100	20
9	3	1.5	1200	60	30
13	4	1.5	1200	140	30
26	5	2.5	1700	100	20
30	6	2.5	1700	100	20
15	7	1.5	2200	140	30
5	8	1.5	1200	140	10
28	9	2.5	1700	100	20
24	10	2.5	1700	100	40
27	11	2.5	1700	100	20
8	12	3.5	2200	140	10
11	13	1.5	2200	60	30
6	14	3.5	1200	140	10
16	15	3.5	2200	140	30
17	16	0.5	1700	100	20
20	17	2.5	2700	100	20
7	18	1.5	2200	140	10
10	19	3.5	1200	60	30
12	20	3.5	2200	60	30
4	21	3.5	2200	60	10
2	22	3.5	1200	60	10
19	23	2.5	700	100	20
22	24	2.5	1700	180	20
23	25	2.5	1700	100	10
21	26	2.5	1700	20	20
14	27	3.5	1200	140	30
3	28	1.5	2200	60	10
1	29	1.5	1200	60	10
18	30	4.5	1700	100	20

The initial (R_{ai}) and after finishing surface roughness values (R_{af}) and the percentage reduction in roughness value ($\%\Delta R_a$) as a response parameter are presented in Table 4.4. As depicted from the Table 4.4, the minimum surface roughness value (R_{af}) was obtained as 63 nm from the initial (R_{ai}) value of 410 nm and the value of the corresponding percentage reduction in surface roughness ($\%\Delta Ra$) comes out to be 84.63%.

Table 4.4: Summary of responses

Std Order	Factors				Initial average roughness value (nm) R_{ai}	After finishing average roughness value (nm) R_{af}	% reduction in roughness value ΔR_a (%)
	I	T	W	A			
1	2.5	1700	100	20	347	79	77.23
2	2.5	1700	100	20	352	77	78.12
3	1.5	1200	60	30	342	120	64.91
4	1.5	1200	140	30	355	184	48.16
5	2.5	1700	100	20	365	81	77.81
6	2.5	1700	100	20	358	89	75.14
7	1.5	2200	140	30	332	137	58.73
8	1.5	1200	140	10	372	178	52.15
9	2.5	1700	100	20	364	87	76.10
10	2.5	1700	100	40	352	160	54.54
11	2.5	1700	100	20	377	82	78.25
12	3.5	2200	140	10	384	69	82.03
13	1.5	2200	60	30	391	118	69.82
14	3.5	1200	140	10	330	102	69.10
15	3.5	2200	140	30	364	73	79.95
16	0.5	1700	100	20	332	143	56.92
17	2.5	2700	100	20	410	63	84.63
18	1.5	2200	140	10	397	130	67.25
19	3.5	1200	60	30	392	98	75.00
20	3.5	2200	60	30	357	72	79.83
21	3.5	2200	60	10	381	69	81.89
22	3.5	1200	60	10	405	111	72.59
23	2.5	700	100	20	369	135	63.41
24	2.5	1700	180	20	385	110	71.43
25	2.5	1700	100	10	342	82	76.02
26	2.5	1700	20	20	362	76	79.00
27	3.5	1200	140	30	349	83	76.22
28	1.5	2200	60	10	356	78	78.10
29	1.5	1200	60	10	341	98	71.26
30	4.5	1700	100	20	396	79	80.00

4.4 Response Surface Regression Analysis

Table 4.4 presents the initial (R_{ai}) and after finishing surface roughness (R_{af}) values and the percentage reduction in roughness value ($\%\Delta R_a$) as a response variable. The percentage reduction in R_a acting as response can be calculated as shown in the Eq. (4.2).

$$\Delta Ra(\%) = [(Ra_i - Ra_f) / Ra_i] * 100 \quad (4.2)$$

Highest order polynomial was selected till the model was not aliased from the calculation of sequential model sum of squares as depicted in the Table 4.5. The highest F-value and the least P-value signifies the addition of quadratic terms to two factor interaction which suggests its suitability. Also the table shows the contribution of increasing complexity to the total model. Table 4.6 showed the lack of fit calculated for all the possible models and insignificant quadratic model is selected.

A quadratic model was selected on the basis of Tables 4.5 and 4.6. All the terms such as I, T, W, A, IT, IW, IA, TW, TA, WA, I^2, T^2, W^2 and A^2 were included initially in the response surface model. Table 4.7 depicted the ANOVA analysis for this model. The F-value of model which lies at 38.66 implies that the model is significant. There is only a 0.01% chance that this large F-value could occur due to noise. Values of 'Prob > F' or p-value greater than 0.05 indicates the model terms are insignificant and the rest are significant terms. The levels having p-value less than or equal to α (significance level) are considered statistically significant. Typical values of α are 0.1, 0.05 and 0.01. The acceptance or rejection of null hypothesis H_0 depends on the agreement of the significance level α. The probability that the null hypothesis is true is α. In decision theory, it is known as a Type I error. To minimize the probability of Type I error which is equal to the significance level α, generally small value of α is chosen.

In the present study, the value of α is taken as 0.05. p-values smaller than 0.05 indicate that terms are significant. In this case I, T, W, A, IW, IA, TA, I^2 and A^2 terms are significant and the rest are insignificant. Model may get improved by removing the insignificant terms. The lack of fit is the variation of the data around the fitted model. The 'F-value' of 4.16 in the 'lack of fit' implies there is 6.44% chance that this large value could occur due to noise.

Table 4.5: Sequential model sum of squares

Source	Sum of squares	DOF	Mean Square	F-Value	p-value Prob > F	Remark
Mean versus total	155088.3	1	155088.3			
Linear versus mean	1980.129	4	495.032	15.73	< 0.0001	
2FI versus linear	297.75	6	49.62	1.92	0.128	
Quadratic versus 2FI	414.207	4	103.55	20.81	< 0.0001	Suggested
Cubic versus quadratic	65.613	9	7.29	4.86	0.03	Aliased
Residual	9	6	1.5			
Total	157855	30	5261.83			

Table 4.6: Lack of fit tests

Source	Sum of Squares	DOF	Mean Square	F Value	Prob > F	Remark
Linear	778.570	20	38.928	24.330	0.0011	
2FI	480.820	14	34.344	21.465	0.0016	
Quadratic	66.613	10	6.661	4.163	0.0644	Suggested
Cubic	1	1	1	0.625	0.4650	Aliased
Pure Error	8	5	1.6			

Table 4.7: ANOVA for percentage reduction in R_a

Source	Sum of Squares	DOF	Mean Square	F-Value	p-value Prob > F	
Model	2692.086	14	192.29	38.65	< 0.0001	Significant
I	988.166	1	988.16	198.65	< 0.0001	
T	580.166	1	580.16	116.63	< 0.0001	
W	240.666	1	240.66	48.38	< 0.0001	
A	51.262	1	51.262	10.30	0.0058	
I^2	115.74	1	115.74	23.26	0.0002	
T^2	2.283	1	2.2831	0.458	0.5084	
W^2	4.715	1	4.7155	0.947	0.3457	
A^2	310.188	1	310.18	62.35	< 0.0001	
IT	2.25	1	2.25	0.452	0.5115	
IW	182.25	1	182.25	36.63	< 0.0001	
IA	64	1	64	12.86	0.0027	
TW	20.25	1	20.25	4.070	0.0619	
TA	25	1	25	5.025	0.0405	
WA	4	1	4	0.804	0.384	
Residual	74.61	15	4.974			
Lack of Fit	66.61	10	6.661	4.163	0.0644	Not significant
Pure Error	8	5	1.6			

Other ANOVA parameters are given in the Table 4.8. 'R^2' is a measure of the amount of reduction in the variability of the response variable from the fitted regression line. In general, the higher the R-squared, the better the model. In the present work, the value comes out to be 0.97. However, higher R-squared value does not imply that the model is a good one as its value can be increased by adding significant or insignificant variables. Thus it is prefer to observe other parameters like adjusted R-squared, predicted R-squared values which are given in the Table 4.8. The predicted R^2 of 0.85 is in reasonable range with the adjusted R^2 of 0.95 i.e. the difference is less than 0.2. 'Adequate precision' measures the signal to noise ratio. A ratio greater than 4 is appropriate. In the present model, this ratio of 23.49 indicates an adequate signal. This model can be used to navigate the design space.

Table 4.8: Other ANOVA parameters

Std. Dev.	2.230302	R^2	0.973032
Mean	71.9	Adj R^2	0.947861
C.V.	3.10195	Pred R^2	0.847209
PRESS	422.7261	Adeq Precision	23.49564

Table 4.9: Factor coefficients

Factor	Coefficient estimate	DOF	Standard error	95% CI low	95% CI high	VIF
Intercept	77.18	1	0.875	75.32	79.05	
I	6.416	1	0.455	5.446	7.387	1
T	4.916	1	0.455	3.946	5.887	1
W	-3.166	1	0.455	-4.137	-2.196	1
A	-1.653	1	0.514	-2.750	-0.555	1.11
I^2	-2.035	1	0.422	-2.935	-1.136	1.03
T^2	-0.285	1	0.422	-1.185	0.613	1.03
W^2	-0.410	1	0.422	-1.310	0.488	1.03
A^2	-4.353	1	0.551	-5.528	-3.178	1.11
IT	-0.375	1	0.557	-1.563	0.813	1
IW	3.375	1	0.557	2.186	4.563	1
IA	2	1	0.557	0.811	3.188	1
TW	1.125	1	0.557	-0.063	2.313	1
TA	-1.25	1	0.557	-2.438	-0.061	1
WA	0.5	1	0.557	-0.688	1.688	1

The high and low values of 95% confidence interval (CI) are shown in the Table 4.9. There are the upper and lower bound of the 95% CI that surrounds the coefficient estimate for the factor. The variance inflation factor (VIF) measures the relative statistical dependency among the variables. If the factor is statistically independent to all the other factors in the model, the VIF comes out to be one. Values greater than 10 indicate that the factors are too correlated together and they are not independent. Depending upon the above calculated coefficients, the final equation in terms of coded factors is given by the Eq. (4.3).

Final equation in terms of coded factors:

$$\text{Percentage reduction in surface roughness, } \%\Delta Ra = 77.19 + 6.42A + 4.92B - 3.17C - 1.65D - 0.37AB + 3.38AC + 2.00AD + 1.13BC - 1.25BD + 0.5CD - 2.04A^2 - 0.29B^2 - 0.41C^2 - 4.35D^2 \quad (4.3)$$

Predictions about the response of each given level of each factor can be made using the equation. By default, the high levels of the factors are coded as +2 and the low levels of

the factors are coded as -2. By comparing the factor coefficients from the coded equation the relative impact of the factors can be identified.

Final equation in terms of actual factors is given in the Eq. (4.4).

$$\text{Percentage reduction in surface roughness, } \%\Delta Ra = 51.11 + 5.43I + 0.01T - 0.35W + 1.37A - 0.00075IT + 0.084IW + 0.21A + 0.000056TW - 0.00025TA + 0.000125WA - 2.036I^2 - 0.0000011T^2 - 0.00026W^2 - 0.043A^2 \quad (4.4)$$

Insignificant terms having p-value greater than 0.05 are neglected to make the model more efficient. There are five insignificant terms which are T^2, W^2, IT, TW and WA. The ANOVA after dropping the insignificant terms is presented in the Table 4.10. The model F-value of 55.04 depicts that the model is significant. There is only 0.01% chance that this large 'F-value' could occur due to noise. The difference between the predicted R-squared value and adjusted R-squared value lies within 0.2 which is an indication of efficient model as depicted in the Table 4.11. The adequate precision value which is a ratio of signal to noise response. Its value of at least 4 should be desirable. In the present model, this value comes out to be 27.19 which is an indication of efficient model. Table 4.12 depicts the range of the factor coefficients that the true coefficient should be found with in this range 95% of the time.

Table 4.10: ANOVA for percentage reduction in R_a after dropping the insignificant terms

Source	Sum of Squares	DF	Mean Square	F-Value	p-value Prob > F	Remark
Model	2659.32	9	295.480	55.035	< 0.0001	significant
I	988.17	1	988.166	184.05	< 0.0001	
T	580.17	1	580.166	108.06	< 0.0001	
W	240.67	1	240.666	44.826	< 0.0001	
A	50.00	1	50.0020	9.3132	0.0063	
I^2	110.13	1	110.130	20.512	0.0002	
A^2	307.01	1	307.014	57.183	< 0.0001	
IW	182.25	1	182.25	33.945	< 0.0001	
IA	64.00	1	64	11.920	0.0025	
TA	25.00	1	25	4.6564	0.0433	
Residual	107.38	20	5.3688			
Lack of Fit	99.38	15	6.6251	4.1407	0.0623	not significant
Pure Error	8.00	5	1.6			
Cor Total	2766.7	29				

Table 4.11: Other ANOVA parameters after model reduction

Std. Dev.	2.31	R^2	0.961
Mean	71.9	Adj R^2	0.943
C.V.	3.22	Pred R^2	0.903
PRESS	267.74	Adeq Precision	27.19

Table 4.12: Factor coefficients after model reduction

Factor	Coefficient Estimate	DOF	Standard Error	95% CI Low	95% CI High	VIF
Intercept	76.549	1	0.679	75.13	77.967	
I	6.416	1	0.472	5.43	7.403	1
T	4.916	1	0.472	3.93	5.903	1
W	-3.166	1	0.472	-4.153	-2.180	1
A	-1.631	1	0.534	-2.746	-0.516	1.11
I^2	-1.957	1	0.432	-2.858	-1.055	1.0
A^2	-4.327	1	0.572	-5.521	-3.133	1.11
IW	3.375	1	0.579	2.166	4.583	1
IA	2	1	0.579	0.791	3.208	1
TA	-1.25	1	0.579	-2.458	-0.042	1

The final equation in terms of coded factors after model reduction is given in Eq. (4.5).

$$\text{Percentage reduction in surface roughness, } \%\Delta Ra = 76.55 + 6.42A + 4.92B - 3.17C - 1.63D + 3.38AC + 2.00AD - 1.25BD - 1.96A^2 - 4.33D^2 \quad (4.5)$$

The final equation in terms of actual factors after model reduction is given in the Eq. (4.6)

$$\%\Delta Ra = 48.02 + 3.76I + 0.015T - 0.29W + 1.49A + 0.08IW + 0.2IA - 0.0002TA - 1.95I^2 - 0.04A^2 \quad (4.6)$$

Percentage contributions of the individual process parameters and their corresponding interactions on the percentage reduction in surface roughness ($\%\Delta R_a$) are shown in the Table 4.13.

Table 4.13: Percentage contribution of individual process parameters and their corresponding interactions in final response value, $\%\Delta R_a$

Source	Sum of squares	Percentage contribution
I	988.17	38.67
T	580.17	22.70
W	240.67	9.42
A	50.00	1.96
I^2	110.13	4.31
A^2	307.01	12.01
IW	182.25	7.13
IA	64.00	2.50
TA	25.00	0.97
Pure Error	8.00	0.31

4.5 Results and Discussion

On the basis of the results of response surface model and Eq. (4.6) which is obtained after regression analysis, the results in terms of effect of current, tool rotation, workpiece rotation and abrasives concentration on the percentage reduction of surface roughness have been observed and computed. The effects of current and tool rotation are found to be maximum. The independent controllable variable effects and interaction effects are found to be significant in ANOVA analysis and therefore discussed below.

4.5.1 Effect of current

The effect of current on percentage reduction in R_a value at tool core rotational speed of 1700 rpm, workpiece rotational speed of 100 rpm and abrasives concentration of 20% is shown in the Fig. 4.1. With increase in the value of current, the percentage reduction in the roughness value increases. Increasing the value of d.c. current supplied to the electromagnetic coil result in the increase of the magnetic flux density in the finishing spot of the MRP fluid. This outcomes in firmly holding of the active abrasives by the carbonyl iron particle (CIPs) chains and thereby result in an increased finishing performance. The finishing at higher current significantly reduces the surface irregularities owing to a higher bonding strength.

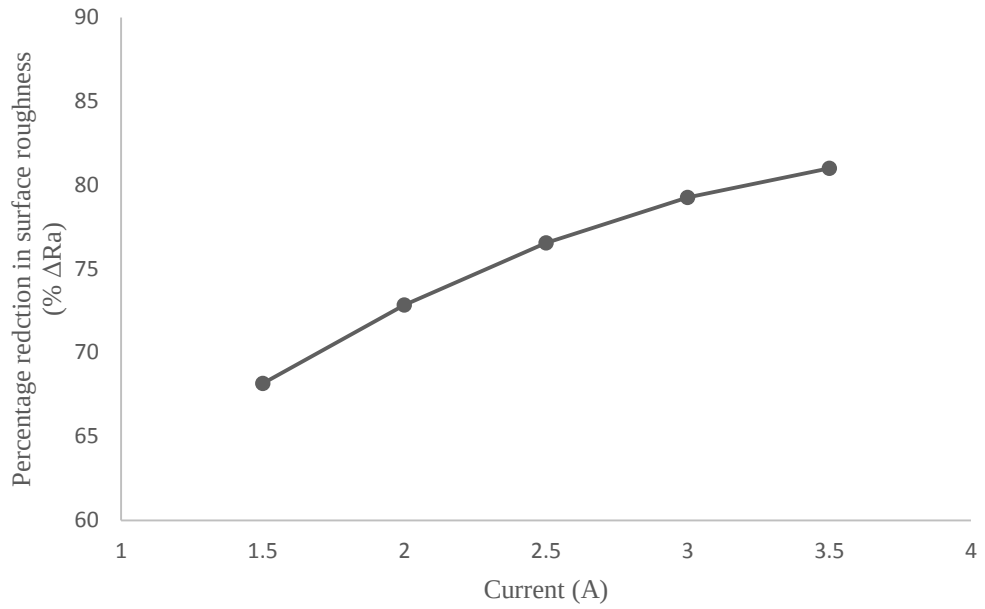

Figure 4.1: Effect of current (A) on percentage reduction in surface roughness (%ΔR_a) at tool rotation of 2200 rpm, workpiece rotation of 60 rpm and 20% abrasives concentration

4.5.2 Effect of tool rotation

The effect of tool core's rotational speed on percentage reduction in R_a value with current at 2.5A, workpiece rotational speed of 100 rpm and abrasives concentration of 20% is shown in the Fig. 4.2. Due to the magnetic flux present at the tool core tip, therefore the CIPs chains stick to it, resulting in the rotation of chains along with the tool. Hence, increase in rotational speed increases the speed of the abrasives. It can be easily depicted from the Fig. 4.2 that at higher tool core rotational speed, higher percentage reduction in roughness was observed. High tool core rotation results in higher relative movement of the active abrasives on the surface of the workpiece which results in drastic increase of the material removal rate. Also because of tool rotation tangential force comes into action which contributes to the resultant force responsible for the overall finishing action.

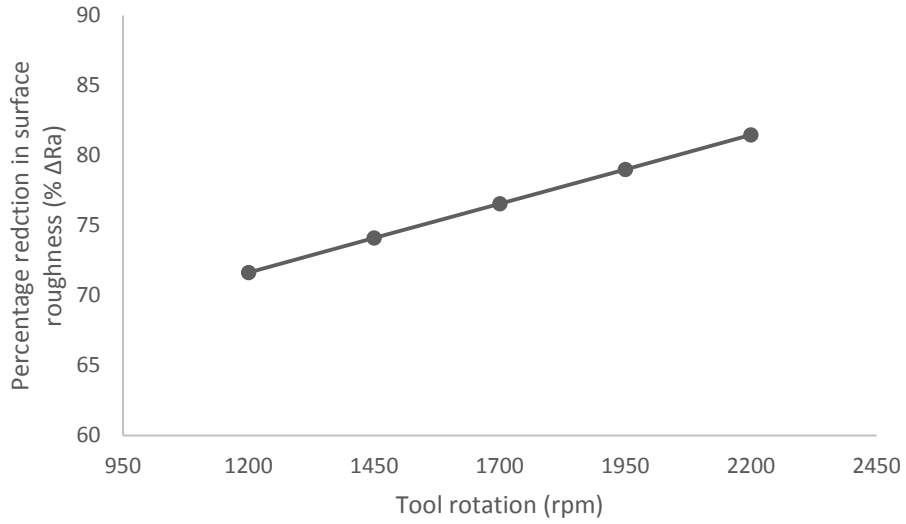

Figure 4.2: Effect of tool rotation (rpm) on percentage reduction in surface roughness (%ΔR_a) at current of 3.5A, workpiece rotation of 60 rpm and 20% abrasives concentration

4.5.3 Effect of workpiece rotational speed

The effect of workpiece rotational speed on percentage reduction in R_a value with current of 2.5A, tool core's rotational speed of 1700 rpm and abrasives concentration of 20% is shown in the Fig. 4.3. There is decreasing trend of percentage reduction in surface roughness (%ΔR_a) with increasing workpiece rotation.

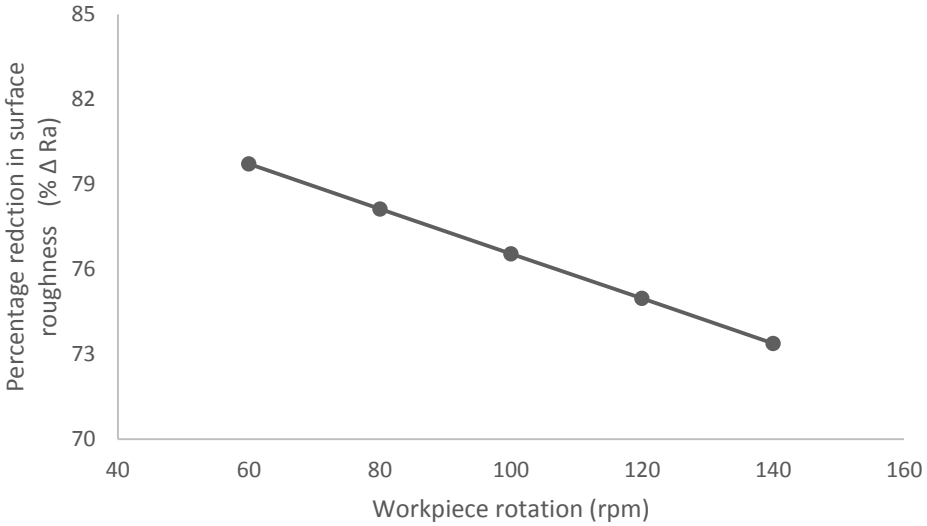

Figure 4.3: Effect of workpiece rotation (rpm) on percentage reduction in surface roughness (%ΔR_a) at current of 3.5A, tool rotation of 1700 rpm and 20% abrasives concentration

The mechanism of material removal at varied workpiece rotation is shown in the Fig. 4.4. As shown in the Fig. 4.4 (a), two vertical forces are involved in the process namely F_1 and F_2 neglecting other horizontal forces. F_1 is the tangential force acted on the workpiece by the abrasive particle due to tool rotation whereas F_2 is the tangential force acted on the abrasive particle by the cylindrical workpiece due to its rotation. Since the tool is rotating at a constant speed of 1700 rpm, therefore the magnitude of tangential force F_1 remains constant. Suppose the workpiece is rotating at slow speed i.e. at 60 rpm, the magnitude of F_2 becomes lesser than F_1. Thus F_1 dominates F_2 resulting in the removal of roughness peaks in the form of micro chips. Now as the workpiece rotational speed starts increasing and so the magnitude of F_2 increases. After some time, a workpiece rotational value will be reached where the magnitude of F_2 completely dominates magnitude of F_1 and thus abrasive particle does not possess enough force to shear off the roughness peaks and it is thus dispersed away from the CIPs chains as shown in the Fig. 4.4 (b). Therefore at higher workpiece rotational speeds, the reduction in surface roughness value R_a is lesser as compared to lower workpiece rotational speeds.

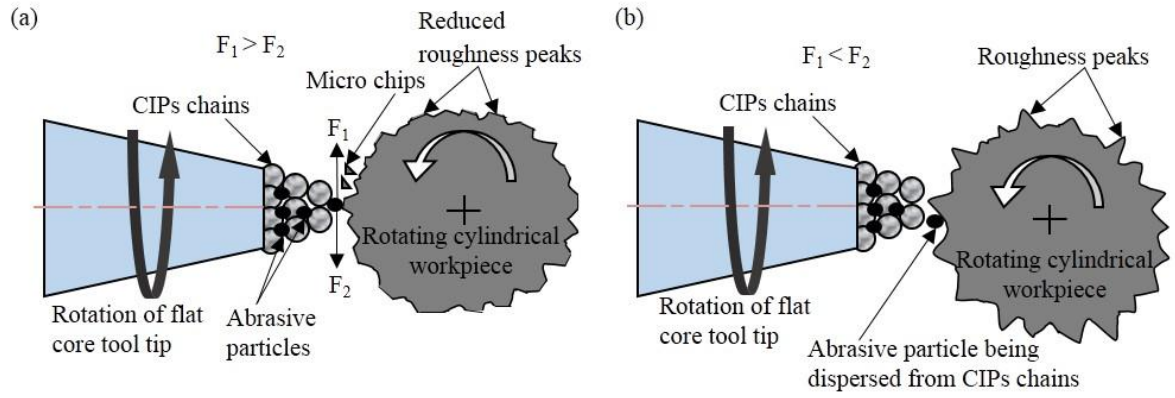

Figure 4.4: Mechanism of material removal (a) at low workpiece rotational speed ($F_1 > F_2$), and (b) at high workpiece rotational speed ($F_1 < F_2$)

4.5.4 Effect of Abrasives concentration

The effect of abrasives concentration on percentage reduction in R_a value with current of 2.5A, tool core's rotational speed of 1700 rpm and workpiece rotational speed of 100 rpm is shown in the Fig. 4.5. Abrasives concentration is of high importance as the abrasives are the sole medium of chipping off the material from the surface of the workpiece. As depicted in the graph, the value of response parameter i.e. percentage reduction in surface roughness

increases up to an abrasives concentration of 20%. However the value of the response variable decreases with further increase in abrasive particles concentration. The rate of the material removed depends on the forces involved. Furthermore, the magnitude of these forces relies mainly on the bonding strength of CIPs. Most of the abrasive particles get trapped in the CIPs chain structure. At high concentration, these particles begin to break the chain structure which ultimately results in decrease in stiffness of MR fluid under shearing action. This outcomes in decreasing of the magnitude of the forces involved and so the material removal rate. However at low concentration, there is less number of particles available to get trapped in the chain structure. It is seen that the optimum concentration is in between 18% and 20% for 20% CIPs concentration.

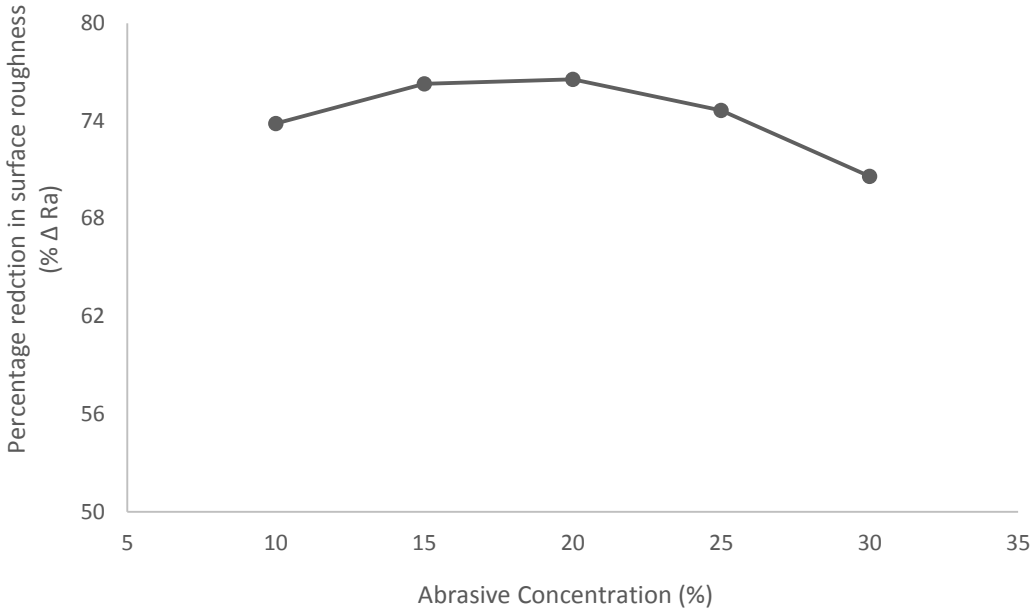

Figure 4.5: Effect of abrasives concentration (%) on percentage reduction in surface roughness (%ΔR_a) at current of 2.5A, tool rotation of 1700 rpm and 60 rpm workpiece rotation.

4.5.5 Effect of interaction of current and workpiece rotation

The effect of interaction of current and workpiece rotation on percentage reduction in R_a value at tool rotational speed of 1700 rpm and 20% abrasives concentration is shown in the Fig. 4.6. In this graph it can be clearly observed that there are two groups of distinct curves one are increasing and other are decreasing. Increasing curves comprised of three workpiece rotational speeds namely 60, 80 and 100 rpm indicate that percentage reduction in surface roughness R_a increase on increasing current. Although these three curves meet at the highest value of percentage reduction in R_a value at 3.5 ampere current but overall curve

corresponding to workpiece rotational speed of 60 rpm i.e. lowest value show high values of percentage reduction in surface roughness in comparison with other increasing curves. Decresiong curves comprised of high workpiece rotational speeds of 120 and 140 rpm indicate that withb increase in current value, the response parameter decreases. Moreover with comparison to increasing curves, these curves are showing much less value of response parameter. Therefore in the end it is concluded that the workpiece with low rotational speed show high value of percentage reduction in surface roughness value R_a with increase in value of current.

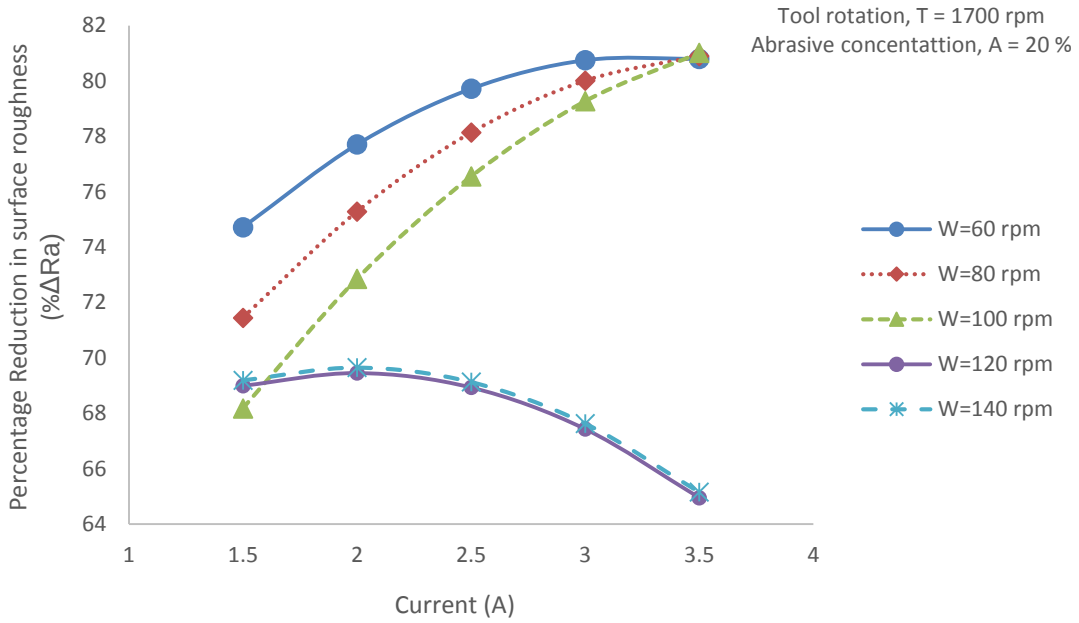

Figure 4.6: Effect of interaction of current and workpiece rotation on percentage reduction in roughness (%ΔR_a)

4.5.6 Effect of interaction of current and abrasives concentration

The effect of interaction of current and abrasives concentration on percentage reduction in R_a value at tool core rotational speed of 1700 rpm and workpiece rotation of 100 rpm is shown in the Fig. 4.7.

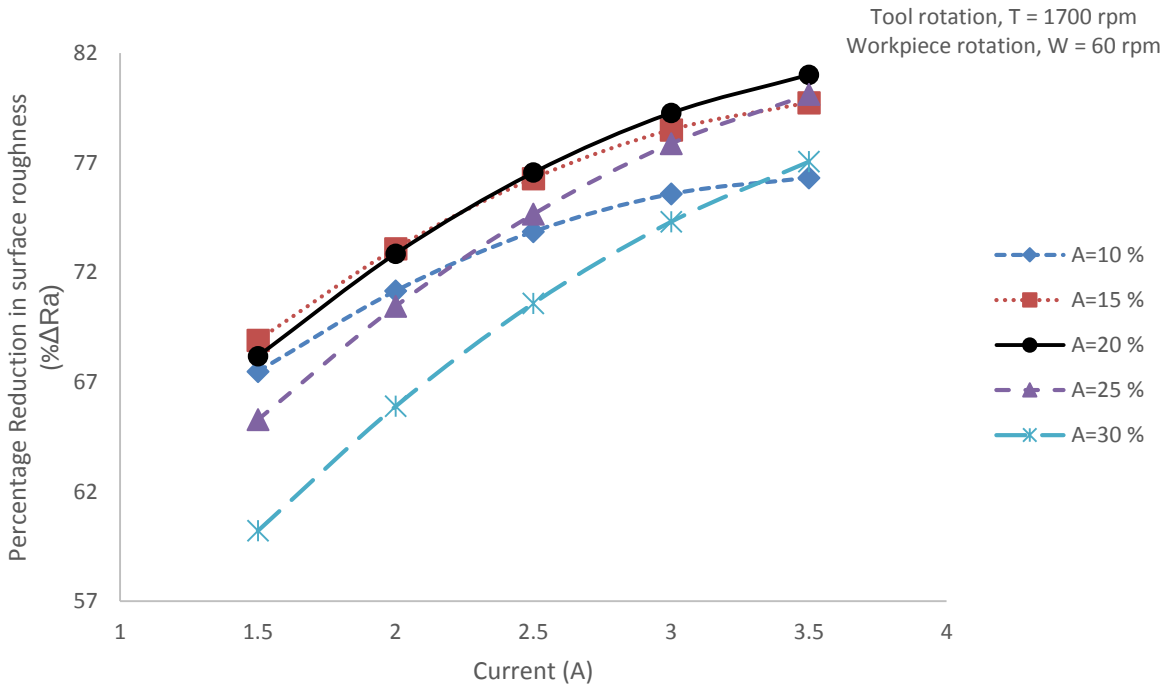

Figure 4.7: Effect of interaction of current and abrasives concentration on percentage reduction in roughness (%ΔR_a)

In this graph, it can be clearly observed that on an individual curve high current value results in higher percentage reduction in Ra value. Since authors interested in more value of response variable, therefore values at 3.5 ampere is considered. Moreover on comparing these curves, the curve corresponding to 20% abrasives concentration show highest value of response parameter followed by the curves corresponding to 15% abrasives concentration and 25% abrasives concentration. The difference of the response variable value on 20% abrasives concentration curve at 3.5 ampere current is small as compared to its neighbour curves corresponding to abrasives concentrations of 15% and 25%. Moreover the curves corresponding to the abrasives concentrations of 10% and 30% show large difference with abrasives concentration curve of 20%. Therefore in the end, it is concluded that abrasives concentration in the range of 15% to 25% result in the high value of response variable.

4.5.7 Effect of interaction of tool rotation and abrasives concentration

The effect of interaction of tool rotation and abrasives concentration on percentage reduction in R_a value at current of 3 ampere and workpiece rotation at 100 rpm is shown in the Fig. 4.8

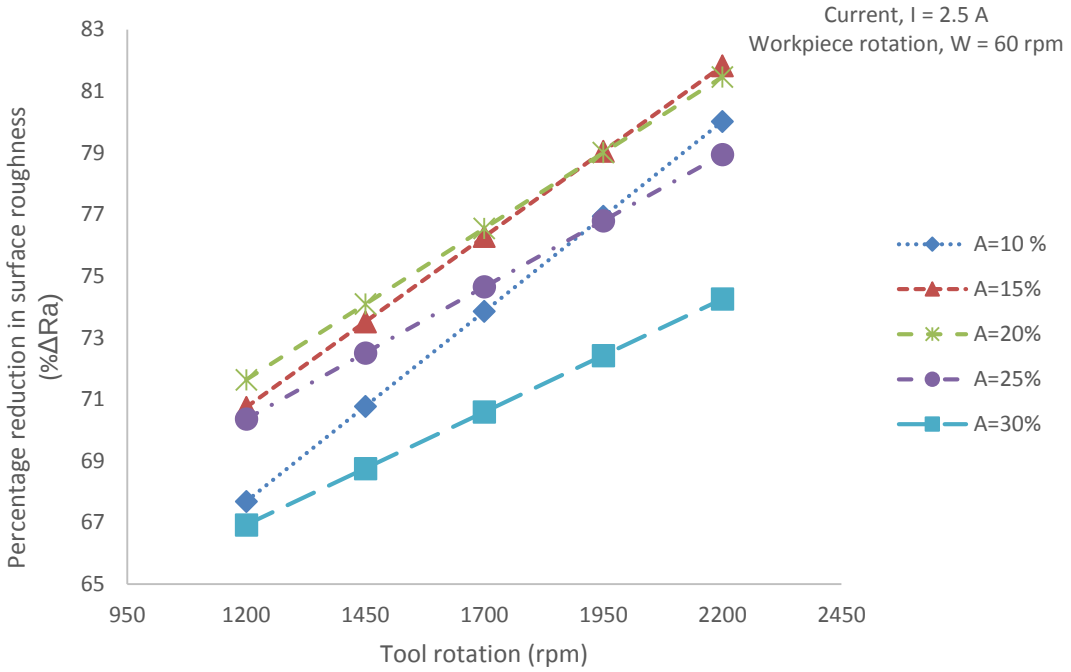

Figure 4.8: Effect of interaction of tool rotation and abrasives concentration on percentage reduction in roughness (%ΔR_a)

It can be clearly observed from the above figure that for a particular value of abrasives concentration, the value of the response variable is maximum for high tool rotation. The response value of 15% and 20% abrasives concentration is nearly same.

The value of the best optimized parameters have been found using Design expert 6.0 software which lies at I = 3.5 A, T = 2200 r/min, W = 60 r/min and A = 20%. These parameters were providing minimum surface roughness value of 52 nm after finishing with the present MR finishing process. The surface roughness profiles of initial and final after finishing with the optimised parameters are shown in Fig. 4.9. The scanning electron microscope (SEM) photographs at 250x optical zoom of the initial surface and the final surface done with optimized parameters are shown in the Fig. 4.10. This clearly indicates the better features of the finished surface as compared with the initial surface of the workpiece. The initial ground surface show scratch marks on the surface because of external cylindrical grinding which are removed later on by using the present magnetorheological finishing process.

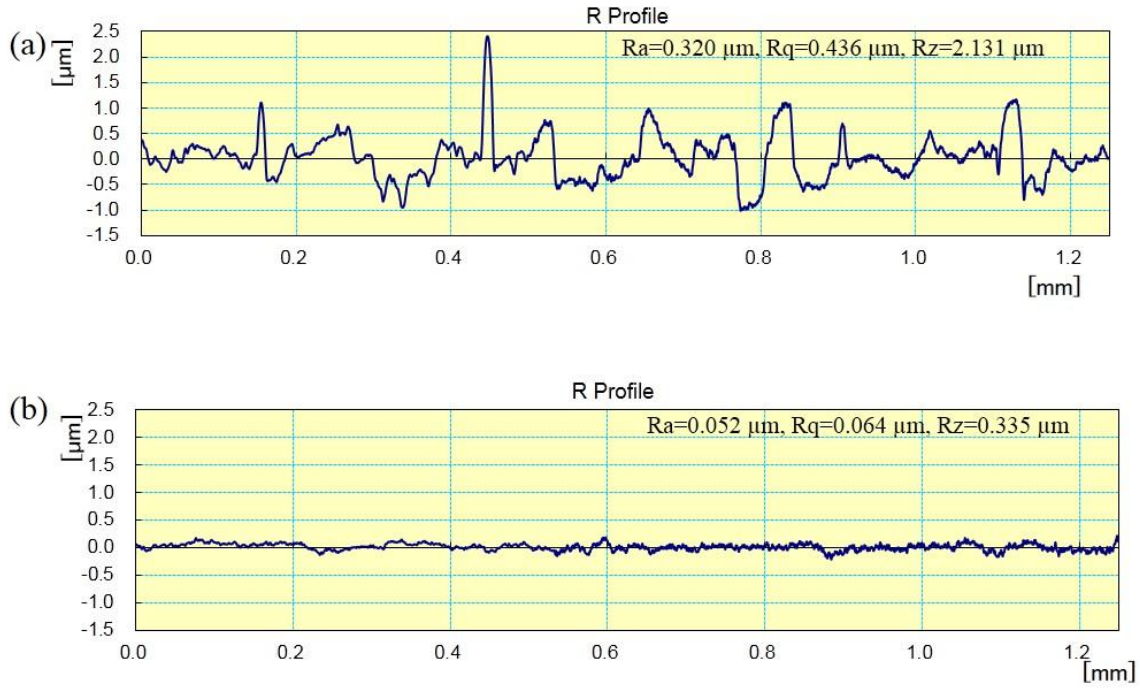

Figure 4.9: Roughness profile from mitutoyo surftest sj-400 (a) before finishing, and (b) after 30 minutes of finishing at optimum parameters

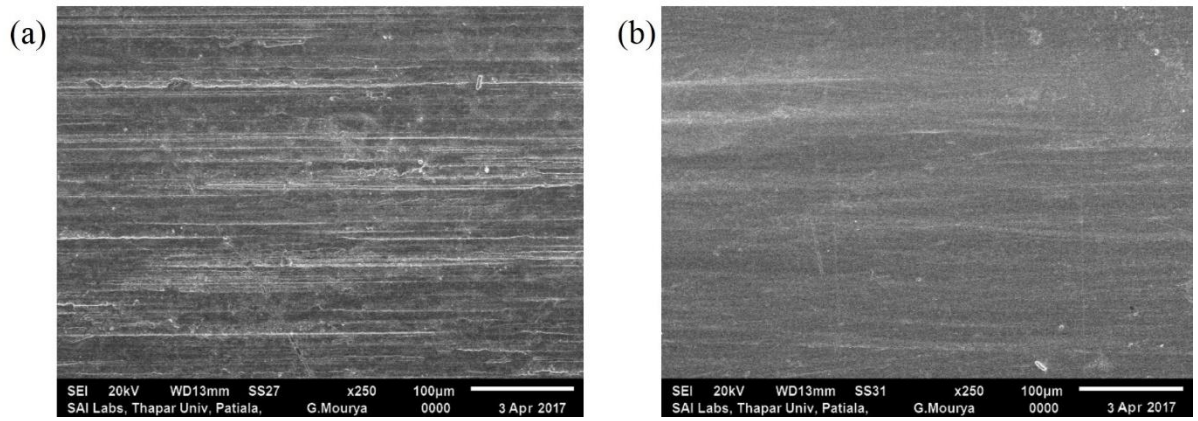

Figure 4.10: SEM images of the workpiece at 250x magnification (a) initial ground surface, (b) workpiece surface after finishing for 30 minutes with optimized parameters

Using the optimizing tool of the Software Design expert 6.0, it was found that the best process parameters are current of 3.5A, 2200 rpm of tool rotation, 60 rpm of workpiece rotation and 20% of abrasives concentration. The final surface roughness value R_a obtained after performing the finishing at these values of the parameters was 52 nm while the initial value of R_a was 320 nm. Thus the percentage reduction in surface roughness ($\%\Delta R_a$) was 83.75%. The predicted value of percentage reduction in surface roughness ($\%\Delta R_a$) can be

calculated by putting the value of optimized parameters in Eq. (4.6). The theoretical value of $\%\Delta R_a$ was found as 88.91% using Eq. (4.6). The comparison between the experimental obtained Ra value and theoretical Ra value is reported in Table 4.14 which showed that the error between the experimental and theoretical values are in good agreement i.e. within 5.16%.

Table 4.14: Comparison between the experimental and theoretical Ra values with the optimized parameters

S.No.	Optimized process parameters				Experimental	Predicted	Error (%)
	I	T	W	A	$\%\Delta R_a$	$\%\Delta R_a$	
1	3.5	2200	60	20	83.75	88.91	-5.16

4.6 Conclusions

The effect of process parameters such as current, tool rotation, workpiece rotation and abrasives concentration on the percentage reduction in roughness was analysed using response surface methodology. The following conclusions are drawn.

- Percentage reduction in surface roughness value ($\%\Delta R_a$) increased with increase in current (I) and tool rotational speed (T). However it decreased with increase in workpiece rotational speed (W).
- $\%\Delta R_a$ increased with increase in abrasives concentration (A) up to 20% but after that it started decreasing with further increase in abrasives concentration.
- Maximum contribution was made by current which was followed by tool rotation, workpiece rotation and finally abrasives concentration.
- Maximum percentage reduction in roughness was observed at current of 2.5A, tool rotational speed of 2700 rpm, workpiece rotational speed of 100 rpm and 20% abrasives concentration. Minimum average roughness of 63 nm from the initial R_a value of 410 nm was obtained in 30 minutes.
- Optimized parameters within the experimental range were found at 3.5A current, 2200 rpm tool rotation, 60 rpm workpiece rotation and 20% abrasives concentration.
- With optimized parameters, the average surface roughness was found as 52 nm from initial value of 320 nm in 30 minutes which correspond to percentage reduction in surface roughness value ($\%\Delta R_a$) of 83.75%.

Chapter 5
Conclusions and Scope of Future Work

5.1 Conclusions

Solid rotating core based magnetorheological finishing process was utilized for finishing of external cylindrical surfaces. The preliminary experimentation was done on external cylindrical surface of mild steel to examine the process capabilities and to study the mechanism of the material removal involved. Furthermore components related to the automobile industry were picked on the finishing requirements basis. The tests revealed the presence of steel of grade C60. Various controllable independent parameters were selected based on the literature review and preliminary experimentation and finally design of experiments was created using Central Composite Design (CCD) which was followed by Optimization of process parameters by the Response Surface Methodology (RSM). The main conclusions are given below.

- Rotating core based magnetorheological finishing process can be an affirmative candidate in finishing external cylindrical surfaces.
- Preliminary experimentation was done on a mild steel shaft in which a minimum surface roughness value R_a found as 40 nm from the initial value of 740 nm in finishing time of 90 minutes while with previously used stationary curved core tool, the R_a value resulted to be 210 nm from the same initial R_a value in 90 minutes.
- Parametric analysis of magnetetorheological finishing on shafts of C60 steel had been done and a theoretical model had been developed to predict the percentage reduction in surface roughness ($\%\Delta R_a$) and error between the experimental and theoretical was found within 4.43%.
- Analysis of Variance (ANOVA) had been successfully applied and it indicated that the maximum contribution to $\%\Delta R_a$ was made by the current (I) which is followed by tool rotational speed (T), workpiece rotational speed (W) and finally abrasives concentration (A).
- Maximum percentage reduction in roughness was observed at current of 2.5A, 2700 rpm tool rotation, 100 rpm workpiece rotation and 20% abrasives concentration with in the given range of experiments. Average roughness value R_a of 63 nm was obtained in 30 minutes.

- The values of the optimized parameters were current at 3.5A, tool rotation at 2200 rpm, workpiece rotation at 60 rpm and 20% abrasives concentration.
- The minimum value of average surface roughness was obtained as 52 nm with the optimized parameters in finishing time of 30 minutes.
- The grinding marks were also removed by the present finishing process with optimized parameters and its verification was done using scanning electron microscopy.

5.2 Scope for Future Work

- Development of setup for finishing tapered workpiece.
- Development of flexible electromagnetic tool on which different tool tips can be fixed and their effect on the finishing process has to be analyzed.
- Effect of other variables like size of Carbon Iron Particles CIPs and abrasive particles can be studied.
- Effect of the size of the workpiece on the performance of the present magnetorheological finishing process and make the process flexible for a particular range of workpiece shaft diameter.

References

Abrão, A.M.; Denkena, B.; Köhler, J.; Breidenstein, B.; Mörke, T.; Rodrigues, P.C.M. (2014) The influence of heat treatment and deep rolling onthe mechanical properties and integrity of AISI 1060 steel. *Journal of Materials Processing Technology*, 214(12), 3020-3030.

Alonso, U.; Ortega, N.; Sanchez, J.A.; Pombo, I.; Izquierdo, B.; Plaza, S. (2015) Hardness control of grind-hardening and finishing grinding by means of area-based specific energy. *International Journal of Machine Tools and Manufacture*, 88, 24-33.

Bedi, T.S.; Singh, A.K. (2016) Magnetorheological methods for nanofinishing–a review. *Particulate Science and Technology*, 34(4), 412-422.

Chang, S.; Farris, T.N.; Chandrasekar, S. (2008) Experimental analysis on evaluation of superfinished surface texture. *Journal of Materials Processing Technology*, 203, 365-371.

Evans, C.J.; Paul, E.; Dornfeld, D.; Lucca, D.A.; Byrne, G.; Tricard, M.; Mullany, B.A. (2003) Material removal mechanisms in lapping and polishing. *CIRP Annals-Manufacturing Technology*, 52(2), 611-633.

Fei, C.; Zuzhi, T.; Xiangfan, W. (2015) Novel process to prepare high-performance magnetorheological fluid based on surfactants compounding. *Materials and Manufacturing Processes*, 30(2), 210-215.

Foeckerer, T.; Zaeh, M.F.; Zhang, O.B. (2013) A three-dimensional analytical model to predict the thermo-metallurgical effects within the surface layer during grinding and grind-hardening. *International Journal of Heat and Mass Transfer*, 56(1), 223-237.

Hashimoto, F.; Yamaguchi, H.; Krajnik, P.; Wegener, K.; Chaudhari, R.; Hoffmeister, H.W.; Kuster, F. (2016) Abrasive fine-finishing technology. *CIRP Annals-Manufacturing Technology*, 65(2), 597-620.

Hyatt, G.A.; Mori, M.; Foeckerer, T.; Zaeh, M.F.; Niemeyer, N.; Duscha, M. (2013) Integration of heat treatment into the process chain of a mill turn center by enabling external cylindrical grind-hardening. *Production Engineering*, 6(7), 571-584.

Jain, V.K. (2008) Abrasive-based nano-finishing techniques: an overview. *Machining Science and Technology*, 12(3), 257-294.

Jang, K.I.; Kim, D.Y.; Maeng, S.; Lee, W.; Han, J.; Seok, J.; Min, B.K. (2012) Deburring microparts using a magnetorheological fluid. *International Journal of Machine Tools and Manufacture*, 53(1), 170-175.

Jermolajev, S.; Heinzel, C.; Brinksmeier, E. (2015) Experimental and analytical investigation of workpiece thermal load during external cylindrical grinding. *Procedia CIRP*, 31, 465-470.

Kim, J.D.; Choi, M.S. (1995) A study on the optimization of the cylindrical lapping process for engineering fine-ceramics (Al_2O_3) by the statistical design method. *Journal of materials processing technology*, 52(2-4), 368-385.

Kordonski, W.; Gorodkin, S.; Behlok, R. (2015) In-line monitoring of (MR) fluid properties. *Journal of Magnetism and Magnetic Materials*, 382, 328-334.

Kumar, H.; Singh, S.; Nanak, G.; Kumar, P. (2013) Magnetic Abrasive Finishing-A Review. *International Journal of Engineering Research & Technology (IJERT)*, 2(3), 2278-0181.

Li, H.N.; Axinte, D. (2016) Textured grinding wheels: A review. *International Journal of Machine Tools and Manufacture*, 109, 8-35.

Liu, M.; Nguyen, T.; Zhang, L.; Wu, Q.; Sun, D. (2015) Effect of grinding-induced cyclic heating on the hardened layer generation in the plunge grinding of a cylindrical component. *International Journal of Machine Tools and Manufacture*, 89, 55-63.

Liu, X.; Wang, L.; Lu, H.; Wang, D.; Chen, Q.; Wang, Z. (2015) A study of the effect of nanometer Fe_3O_4 addition on the properties of silicone oil-based magnetorheological fluids. *Materials and Manufacturing Processes*, 30(2), 204-209.

Maan, S.; Singh, G.; Singh, A.K. (2017) Nano-surface-finishing of permanent mold punch using magnetorheological fluid-based finishing processes. *Materials and Manufacturing Processes*, 32(9), 1004-1010.

Malkin, S.; Guo, C. (2007) Thermal analysis of grinding. *CIRP Annals-Manufacturing Technology*, 56(2), 760-782.

Mishra, V.; Goel, H.; Mulik, R.S.; Pandey, P.M. (2014) Determining work-brush interface temperature in magnetic abrasive finishing process. *Journal of Manufacturing Processes*, *16*, 248–256.

Montgomery, D.C. (2001) Design and analysis of experiments. 5th ed., John Wiley & Sons Inc, New York.

Nguyen, T.; Zhang, L.C. (2011) Realisation of grinding-hardening in workpieces of curved surfaces—Part 1: Plunge cylindrical grinding. *International Journal of Machine Tools and Manufacture*, 51(4), 309-319.

Nguyen, T.; Liu, M.; Zhang, L.; Wu, Q.; Sun, D. (2014) An investigation of the grinding-hardening induced by traverse cylindrical grinding. *Journal of Manufacturing Science and Engineering*, 136(5), 051008.

Neagu-Ventzel, S.; Cioc, S.; Marinescu, I. (2006) A wear model and simulation of superfinishing process: analysis for the superfinishing of bearing rings. *Wear*, 260(9), 1061-1069.

Sidpara, A.; Das, M.; Jain, V.K. (2009) Rheological characterization of magnetorheological finishing fluid. *Materials and Manufacturing Processes*, 24 (12), 1467–1478.

Sidpara, A.; Jain, V.K. (2011) Experimental investigations into forces during magnetorheological fluid based finishing process. *International Journal of Machine Tools and Manufacture*, 51(4), 358-362.

Sidpara, A.; Jain, V.K. (2012) Theoretical analysis of forces in magnetorheological fluid based finishing process. *International Journal of Mechanical Sciences*, 56(1), 50-59.

Sidpara, A.; Jain, V.K. (2013) Analysis of forces on the freeform surface in magnetorheological fluid based finishing process. *International Journal of Machine Tools and Manufacture*, 69, 1-10.

Singh, A.K.; Jha, S.; Pandey, P.M. (2011) Design and development of nanofinishing process for 3D surfaces using ball end MR finishing tool. *International Journal of Machine Tools and Manufacture*, 51(2), 142-151.

Singh, A.K.; Jha, S.; Pandey, P. M. (2012) Nanofinishing of fused silica glass using ball-end magnetorheological finishing tool. *Materials and Manufacturing Processes*, 27(10), 1139-1144.

Singh, A.K.; Jha, S.; Pandey, P.M. (2013) Mechanism of material removal in ball end magnetorheological finishing process. *Wear*, 302(1), 1180-1191.

Singh, D.K.; Jain, V.K.; Raghuram, V. (2004) Parametric study of magnetic abrasive finishing process. *Journal of materials processing technology*, 149(1), 22-29.

Singh, G.; Singh, A.K.; Garg, P. (2016) Development of magnetorheological finishing process for external cylindrical surfaces. *Materials and Manufacturing Processes*, 32(5), 581-588.

Zarudi, I.; Zhang, L.C. (2002) Mechanical property improvement of quenchable steel by grinding. *Journal of materials science*, 37(18), 3935-3943.

Web References

W.1 Crankshaft Polishing, www.enginebuildermag.com/1998/09/crankshaft-polishing-make-sure-the-journals-on-the-crankshaft-are-properly-polished/ (08.02.2017)

LIST OF PUBLICATIONS

SCI Journal:

Singh, M.; **Singh, A.**; Singh, A.K. (2017) A Rotating Core Based Magnetorheological Nano-Finishing Process for External Cylindrical Surfaces. *Materials and Manufacturing Processes*, doi: 10.1080/10426914.2017.1328116.
Status: ***Online published***
Publisher: Taylor and Francis
Impact factor: 1.419

International Conference:

Singh, A.; Singh, A.K. (2016) A Review on Advanced Abrasive Finishing Process for External Cylindrical Surfaces. IVth International Conference on Production and Industrial Engineering, CPIE-2016, Held on 19-21st December, Dr B R Ambedkar National Institute of Technology, Jalandhar.
Status: ***Accepted***